



Limit theorems and localization of three-state quantum walks on a line defined by generalized Grover coins

Amrita Mandal ^{1,*} Rohit Sarma Sarkar,^{1,†} Shantanav Chakraborty,^{2,3,‡} and Bibhas Adhikari ^{1,§}

¹Department of Mathematics, Indian Institute of Technology Kharagpur, Kharagpur 721302, India

²Centre for Quantum Science and Technology, International Institute of Information Technology, Hyderabad 500032, India

³Centre for Security, Theory and Algorithmic Research, International Institute of Information Technology, Hyderabad 500032, India



(Received 2 May 2022; accepted 20 September 2022; published 4 October 2022)

In this article, we undertake a detailed study of the limiting behavior of a three-state discrete-time quantum walk on a one-dimensional lattice with generalized Grover coins. Two limit theorems are proved and consequently we show that the quantum walk exhibits localization at its initial position for a wide range of coin parameters. Finally, we discuss the effect of the coin parameters on the peak velocities of probability distributions of the underlying quantum walks.

DOI: [10.1103/PhysRevA.106.042405](https://doi.org/10.1103/PhysRevA.106.042405)

I. INTRODUCTION

Quantum walks, the quantum analog of classical random walks [1], represent a universal model for quantum computation [2,3]. Besides being a useful primitive to design quantum algorithms [4–7], quantum walks also provide a useful framework to model transport in quantum systems [8–10]. Just as in the classical scenario, quantum walks can be defined in both discrete time and in continuous time [11–13]. Often for several of the aforementioned applications, studying the long-time behavior of both discrete-time and continuous-time quantum walks is extremely crucial. Quantum evolutions are unitary and hence quantum walks do not naturally converge to a limiting distribution, unlike classical random walks. However, for a quantum walk, one can define the limiting distribution as the long-time average probability distribution of finding the walker in each node of the graph. This long-time behavior of quantum walks has been fundamental to demonstrate the speedup of several quantum algorithms [4,14,15], to prove the equivalence between the circuit and Hamiltonian models of quantum computing [16,17], and also to understand the phenomenon of mixing of quantum walks [1,18–20]. Consequently, it is important to develop a more comprehensive understanding of the limiting distributions of the various quantum walks and to highlight the features that distinguish them from their classical counterparts.

Localization has been widely studied in the context of discrete-time quantum walks and its precise definition varies across articles (for example, see Refs. [21–26] and the references therein). The probability of finding the walker at a fixed lattice point converges to zero after infinite long time in the case of a Hadamard walk on a line with two inner

states [27]. In this paper our goal is to study the limiting distribution and the localization phenomena for the coined three-state discrete-time quantum walk on a line. We consider two distinct families of parametrized coin operators which we introduced in Ref. [28]: one that includes the widely used Grover coin as a special case, while the other does not. In particular, for this graph, we demonstrate, localization on a general family of coins that does not include the Grover coin.

Inui *et al.* derived the first long-time limit theorem for the three-state quantum walk on a line with a Grover coin (generally referred to as the Grover walk) and showed that the probability of finding the particle at the origin does not converge to zero after infinite time steps, demonstrating localization [23]. On the other hand, the three-state quantum walk with an asymmetrical jump and three-state quantum walk on a triangular lattice, both using the Grover coin, do not exhibit localization [22,29]. The probability of staying at the initial position also vanishes for some special set of escaping initial states in the case of a two-dimensional Grover walk on the Cartesian lattice, leading to partial trapping [21]. Furthermore, there exists quantum coins for such escaping states (corresponding to strong trapping) [25]. In Ref. [30], the authors have classified explicitly the coins leading to the trapping effect for a walk on a two-dimensional square lattice based on the existence or nonexistence of an escaping state.

Attempts have been made to generalize the Grover walk in the literature by considering parametric coin operators that contain the Grover matrix for some specific values of the parameters [21,28,31,32]. Discrete-time quantum walks with a generalized Grover coin are generally referred to as generalized Grover walks (GGWs). One of the endeavors of the community has been to understand the dynamics of GGWs in order to distinguish them from their classical counterparts [28,33,34]. The dependence of the underlying quantum walk dynamics on the values of the coin parameters has been explored in Ref. [35]. The limit distribution of a four-state quantum walk with a parametric coin has been investigated in Ref. [33]. The authors of Ref. [36] have provided

*mandalamrita55@gmail.com

†rohit15sarkar@yahoo.com

‡shchakra@iiit.ac.in

§bibhas@maths.iitkgp.ac.in

analytical results for the asymptotic value of the return probability and discuss the localization of a two-state one-dimensional Discrete-time coined quantum walks (DTQWs) as $t \rightarrow \infty$. In Ref. [31] Štefaňák *et al.* have introduced two families of parametric coin operators: one by deforming the eigenvalues and the other by deforming the eigenvectors of the Grover coin. Furthermore, in Ref. [37] Štefaňák *et al.* have presented a rigorous analysis of the limiting behavior of these coined walks and the role of eigenstates for the localization phenomena. In Ref. [34] we have explored the localization property of four state quantum walks on two-dimensional lattices with generalized Grover coins.

In terms of GGWs, it is undoubtedly challenging to find the parametric coin matrices that preserve the property of Grover walks. With an appropriate choice of coin operator from the generalized coin collections, the result regarding localization at a position may help us to design effective quantum algorithms based on the corresponding quantum walk [38]. Furthermore, it is interesting to ask whether it is indeed possible to study the long-time dynamics of discrete-time quantum walks using a class of parametric coin operators that do not include the Grover coin. Can such quantum walks exhibit localization? In this article, we make inroads towards answering these questions by considering two families of parametric orthogonal coin operators of dimension 3×3 . Mathematically, these coin operators are a linear sum of permutation matrices and hence they can have convenient quantum circuit representation [39]. These coins have been used recently to study properties of quantum walks dynamics such as periodicity of evolution [28]. In this article, we derive the long-time-limit probability distributions and study the localization of three-state DTQWs with these families of parametric coin operators. Using this limiting value of the probability measure we are able to justify localization phenomena at a vertex for a given initial state.

Furthermore, the spread of the quantum walk wave function on a line can be modeled using the theory of wave front propagation [40–42]. In this framework, Ref. [31] analyzed the peak velocities of the wave functions of two GGWs and explored the dependence of the coin parameter on the rate of propagation of the walk through the line. Furthermore, the localization of the wave function is dependent on the eigenvalues of the evolution operator that are independent of the wave number (constant). These correspond to the peak of the probability distribution which does not propagate, ensuring localization. Based on the constant eigenvalues of the evolution operator, a necessary and sufficient condition is obtained in Ref. [26] for quantum walks on infinite lattices, corresponding to a periodic transition operator that does not localize at a vertex.

In this article, following Ref. [37], we also find the peak velocities of the wave function as a function of the parameters corresponding to the general families of coin operators that we have considered. We revisit the localization phenomena from the aspect of zero traveling velocity of one of the peaks. Consequently, we obtain new families of 3×3 generalized Grover coin operators, preserving localization, which is different from the two classes mentioned in Ref. [31]. This answers a question posed by Štefaňák *et al.* in Ref. [31]. In this work we note that the permutation coins play a key role in the

behavioral changes of probability distribution at a time and sign changes of group velocities. These observations make the proposed walk intriguingly different from the existing GGWs in the literature.

The organization of this paper is as follows: In Sec. II we formally define the quantum walk we consider, namely, three-state DTQWs on a line with parametric coin operators. We present two limit theorems on probability distributions at infinite time steps and establish the localization property in Sec. III. In Sec. IV we determine the right- and left-traveling peak velocities of the probability distribution as a function of coin parameter and discuss the impact of the peak velocities on the localization phenomena of the walks. Finally, we conclude this article with some problems that can be considered in the near future.

II. THREE-STATE WALK ON A LINE AND GENERALIZED GROVER COINS

In this section we review three-state quantum walks on a line [23,31] and we briefly discuss generalized Grover coins of dimension 3×3 that were recently introduced in the literature [28].

Discrete time coined quantum walks (DTQWs) are defined on the Hilbert space $\mathcal{H} = \mathcal{H}_p \otimes \mathcal{H}_c$, where \mathcal{H}_p is the position space and \mathcal{H}_c is the coin space. The Hilbert space \mathcal{H}_p is considered as separable and is isomorphic to $l^2(\mathbb{Z})$, the Hilbert space of all square summable functions on \mathbb{Z} . Hence the superposition of the canonical basis vectors subject to the unit norm condition form the position state vector $|m\rangle \in \mathcal{H}_p$ for the position $m \in \mathbb{Z}$ [13]. Otherwise, in a more conventional way we can say that $\mathcal{H}_p = \text{Span}\{|m\rangle | m \in \mathbb{Z}\}$ [31,43].

At every step the intrinsic behavior of the quantum particle allows it to move to the right or to the left or stay at its current position. Hence the dimension of \mathcal{H}_c is three, which is the number of internal degrees of freedom (called chirality) of the particle at each step. The vector of the standard basis assigned to each of these three displacements spans the space \mathcal{H}_c , i.e., $\mathcal{H}_c = \text{Span}\{|1\rangle, |2\rangle, |3\rangle\}$, where $\{|l\rangle | l = 1, 2, 3\}$ is the canonical ordered basis of \mathbb{C}^3 . Thus the total state space $\mathcal{H} = \text{Span}\{|m\rangle \otimes |l\rangle | m \in \mathbb{Z}, l \in \{1, 2, 3\}\}$ and is isomorphic to $l^2(\mathbb{Z}) \otimes \mathbb{C}^3$ [44].

One single step of a DTQW is described by a unitary operator $U = \mathbf{S}(I \otimes C)$, where I is the identity operator acting on \mathcal{H}_p , C is the coin operator acting on the space \mathcal{H}_c while \mathbf{S} is the conditional shift operator, allows the walker to transition into the next step, controlled by the state of the coin register. The operator \mathbf{S} , acting at a particle in position $m \in \mathbb{Z}$ results in

$$\begin{aligned} \mathbf{S} = & \sum_{m \in \mathbb{Z}} (|m-1\rangle \langle m| \otimes |1\rangle \langle 1| + |m\rangle \langle m| \otimes |2\rangle \langle 2| \\ & + |m+1\rangle \langle m| \otimes |3\rangle \langle 3|). \end{aligned}$$

The state vector $|\psi(t)\rangle \in \mathcal{H}$ of the walker after t time steps is given by

$$\begin{aligned} |\psi(t)\rangle &= U |\psi(t-1)\rangle = U^t |\psi(0)\rangle \\ &= \sum_{m \in \mathbb{Z}} \sum_{l \in \{1,2,3\}} \psi_l(m, t) |m\rangle \otimes |l\rangle, \end{aligned} \quad (1)$$

where the product state of initial position state and initial coin state is the initial state vector $|\psi(0)\rangle \in \mathcal{H}$ and $\psi_l(m, t)$ is the probability amplitude at time t and at the position m , with coin state $|l\rangle$, $l \in \{1, 2, 3\}$. Then at time t and at $m \in \mathbb{Z}$ the probability amplitude vector for chirality state being left, center, or right is

$$|\psi(m, t)\rangle = [\psi_1(m, t), \psi_2(m, t), \psi_3(m, t)]^T. \quad (2)$$

Therefore we write

$$|\psi(t)\rangle = [\dots, |\psi(-1, t)\rangle, |\psi(0, t)\rangle, |\psi(1, t)\rangle, \dots]^T.$$

Now for a complex-valued function $f \in L^2(\mathbb{Z})$, its discrete Fourier transform $\mathbf{f}: \mathbb{I} \rightarrow \mathbb{C}$ is defined as $\mathbf{f}(k) = \sum_{m \in \mathbb{Z}} f(m) e^{imk} \in L^2(\mathbb{I})$, where $\mathbb{I} = [-\pi, \pi]$ and $L^2(\mathbb{I})$ is the Hilbert space consisting of all square integrable functions on \mathbb{I} . Thus the Fourier transform from $L^2(\mathbb{Z})$ to $L^2(\mathbb{I})$ extends to

$$\begin{aligned} |\Psi(k, t+1)\rangle &= \sum_{m \in \mathbb{Z}} [|1\rangle \langle 1| C |\psi(m-1, t)\rangle + |2\rangle \langle 2| C |\psi(m, t)\rangle + |3\rangle \langle 3| C |\psi(m+1, t)\rangle] e^{imk} \\ &= \sum_{m \in \mathbb{Z}} e^{ik} |1\rangle \langle 1| C |\psi(m-1, t)\rangle e^{i(m-1)k} + |2\rangle \langle 2| C |\psi(m, t)\rangle e^{imk} + e^{-ik} |3\rangle \langle 3| C |\psi(m+1, t)\rangle e^{i(m+1)k} \\ &= (e^{ik} |1\rangle \langle 1| C + |2\rangle \langle 2| C + e^{-ik} |3\rangle \langle 3| C) |\Psi(k, t)\rangle \\ &= \text{diag}(e^{ik}, 1, e^{-ik}) C |\Psi(k, t)\rangle. \end{aligned}$$

Let $\tilde{U}(k) = D(k)C$ for $D(k) = \text{diag}(e^{ik}, 1, e^{-ik})$. Then from above the time evolution in momentum space is given as [43,45]

$$|\Psi(k, t)\rangle = \tilde{U}(k) |\Psi(k, t-1)\rangle = \tilde{U}^t(k) |\Psi(k, 0)\rangle. \quad (4)$$

Let the eigenvalues of the unitary operator $\tilde{U}(k)$ be of the form $e^{iw_j(k)}$ with the corresponding eigenvector $|v_j(k)\rangle$ for $j \in \{1, 2, 3\}$. Then the vector of probability amplitudes can be determined by Eqs. (3) and (4) as follows:

$$|\psi(m, t)\rangle = \frac{1}{(2\pi)} \int_{k \in (-\pi, \pi]} e^{-ikm} |\Psi(k, t)\rangle dk = \sum_{j=1}^3 \frac{1}{(2\pi)} \int_{k \in (-\pi, \pi]} e^{i[-km + w_j(k)t]} \langle v_j(k) | \Psi(k, 0) \rangle |v_j(k)\rangle dk. \quad (5)$$

From (1), the probability of finding the walker at time t and at position m is

$$\begin{aligned} P(m, t) &= \langle \psi(m, t) | \psi(m, t) \rangle \\ &= |\psi_1(m, t)|^2 + |\psi_2(m, t)|^2 + |\psi_3(m, t)|^2, \quad (6) \end{aligned}$$

and it can be derived from Eq. (5). Whereas, the probability $P(0, t)$ of finding the walker at position $m = 0$ after t time steps, which is also called the return probability of the walker to the initial position 0, can be evaluated as $P(0, t) = \langle \psi(0, t) | \psi(0, t) \rangle$. Note that, if the walk starts at $m = 0$ and is localized there, then from Eq. (1), we get that

$$|\psi(0)\rangle = \sum_{l=1}^3 \psi_l(0, 0) |0\rangle \otimes |l\rangle,$$

whereas the other probability amplitudes $\psi_l(m, 0) = 0$ for $m \neq 0$. Hence from Eq. (3) we have that $|\Psi(k, 0)\rangle = |\psi(0, 0)\rangle$. We assume that the initial state of the walker is at the origin. Thus, the initial quantum states are determined by $|\psi(0, 0)\rangle = [\alpha, \beta, \gamma]^T$, where $\alpha, \beta, \gamma \in \mathbb{C}$ and $|\alpha|^2 + |\beta|^2 + |\gamma|^2 = 1$.

the Fourier transformation of $|\psi(m, t)\rangle$ as

$$|\Psi(k, t)\rangle = \sum_{m \in \mathbb{Z}} |\psi(m, t)\rangle e^{ikm}, \quad (3)$$

where $|\Psi(k, t)\rangle = [\Psi_1(k, t), \Psi_2(k, t), \Psi_3(k, t)]^T$, $\Psi_l(k, t) = \sum_{m \in \mathbb{Z}} \psi_l(m, t) e^{ikm}$, $l = 1, 2, 3$ for $k \in \mathbb{I}$. The inverse Fourier transformation is given as

$$|\psi(m, t)\rangle = \frac{1}{(2\pi)} \int_{[-\pi, \pi]} e^{-ikm} |\Psi(k, t)\rangle dk.$$

Now we obtain the time evolution of $|\psi(m, t)\rangle$ from Eqs. (1) and (2) as

$$\begin{aligned} |\psi(m, t+1)\rangle &= |1\rangle \langle 1| C |\psi(m-1, t)\rangle + |2\rangle \langle 2| C |\psi(m, t)\rangle \\ &\quad + |3\rangle \langle 3| C |\psi(m+1, t)\rangle, \end{aligned}$$

where C is the coin operator. Then the following holds from (3):

We emphasize that the localization phenomena is extensively studied in the literature for DTQWs on different topologies of the underlying system with a variety of coin operators, as mentioned in Sec. I. However, the mathematical definition of localization associated with the probability measure of finding the walker at a vertex differs across articles. For example, in Ref. [21], the positive value of the total time-averaged probability $\lim_{T \rightarrow \infty} \frac{1}{T} \sum_{t=0}^{T-1} P(m, t)$, $T \geq 1$ is considered as the condition for localization, whereas in Ref. [46] a positive value of $\sum_{m \in \mathbb{Z}} \lim_{t \rightarrow \infty} P(m, t)$ is taken to be the criterion for localization. Indeed, it has been shown that the localization phenomena at the initial position depends on the initial state of the walker [23]. In this paper, we follow the localization criterion outlined in Ref. [47]. Thus we consider the localization of a DTQW at a location m corresponding to an initial state if $\lim_{t \rightarrow \infty} P(m, t) > 0$. A computable formula of this limiting value is obtained in terms of the coin parameters and a generic initial state. Therefore, the limiting value can be obtained with a given initial state and the coin parameters and consequently, the localization phenomena can be tested. For completeness, we also classify all the initial states

for which the proposed walks exhibit localization. Finally we provide a condition based on the coin parameters satisfying which the proposed walks show localization in the sense of Ref. [46].

$$\mathcal{X} = \left\{ \begin{bmatrix} x & y & 1-x-y \\ 1-x-y & x & y \\ y & 1-x-y & x \end{bmatrix} : x^2 + y^2 - x - y + xy = 0, -\frac{1}{3} \leq x \leq 1 \right\},$$

$$\mathcal{Y} = \left\{ \begin{bmatrix} x & y & -1-x-y \\ -1-x-y & x & y \\ y & -1-x-y & x \end{bmatrix} : x^2 + y^2 + x + y + xy = 0, -1 \leq x \leq \frac{1}{3} \right\}.$$

It is easy to check that the Grover coin is an element of \mathcal{X} by setting $x = -1/3$ and $y = 2/3$; whereas the negative of the Grover coin is a member of \mathcal{Y} setting $x = 1/3$ and $y = -2/3$. It is also shown in Ref. [28] that \mathcal{X} and $\mathcal{X} \cup \mathcal{Y}$ both form groups under matrix multiplication. Furthermore, we consider one-parameter trigonometric parametrization of \mathcal{X} and \mathcal{Y} as \mathcal{X}_θ and \mathcal{Y}_θ , respectively (see Sec. III). Then it is obvious that, if $A(\theta) \in \mathcal{X}_\theta \cup \mathcal{Y}_\theta$, then $[A(\theta)]^{-1} = [A(\theta)]^T = A(-\theta)$ where $\theta \in [-\pi, \pi]$. Another salient feature of these parametric orthogonal matrices is that these are permutative matrices; that is, any row of any such matrix is a permutation of any other row, a combinatorial structure of the Grover matrix. Besides, matrices in $\mathcal{X} \cup \mathcal{Y}$ can be expressed as a linear sum of permutation matrices. Consequently, these coins can conveniently be implemented by parametrized quantum circuits [48]. Finally, we establish from the numerical computation that $\lim_{t \rightarrow \infty} P(m, t)$ at the initial position m is equal for the coin operators $A(\theta)$ and its inverse $A(-\theta)$.

As mentioned in the introduction, attempts have been made in the literature to study coined quantum walks by generalizing the Grover diffusion matrix with parametric unitary matrices. However, the existing classes of parametric coins do not have any algebraic structure such as a group structure. This makes the proposed classes of coins significantly different from the existing parametric coins in the literature. Moreover, note that $\text{Det}(A) = 1$ if $A \in \mathcal{X}$ and $\text{Det}(A) = -1$ if $A \in \mathcal{Y}$ (see Ref. [28]). Hence the matrices in \mathcal{X} and \mathcal{Y} belong to different connected components in the Lie group formed by orthogonal matrices of order 3.

In the next two sections we determine the limit laws of the probability distribution for infinite time steps. Besides, we discuss the localization phenomena of the walks from two different aspects: existence of the nonzero return probability $\lim_{t \rightarrow \infty} P(m, t)$ and the zero velocity of probability distribution peak of the particle to stay at the position $m = 0$ on the line.

III. LIMIT THEOREMS FOR WALKS WITH GENERALIZED GROVER COINS

The asymptotic probability distribution and the localization of three-state walks on one- and two-dimensional lattices with parametric coin operators have been studied [46,49]. In this section, we consider the three-state walks on a line with parametric coin operators $C \in \mathcal{X} \cup \mathcal{Y}$. We present the limit

A. Generalized Grover coins

In this work we consider 3×3 parametric coin operators to describe the three-state DTQWs on the line. In particular, we choose $C \in \mathcal{X}$ and $C \in \mathcal{Y}$ [28], where

value of the probability that a walker can be found at a vertex on \mathbb{Z} for long time. In addition, we show the localization phenomena of these walks.

A. Coins from \mathcal{X}

The evolution operator of three-state walk with generalized Grover coin in Fourier domain is given by $\tilde{U}_X(k) = D(k)C$, where $C \in \mathcal{X}$ and $k \in (-\pi, \pi]$. Indeed, we write explicitly

$$\tilde{U}_X(k) = \begin{bmatrix} xe^{ik} & ye^{ik} & (1-x-y)e^{ik} \\ 1-x-y & x & y \\ ye^{-ik} & (1-x-y)e^{-ik} & xe^{-ik} \end{bmatrix}, \tag{7}$$

where $x^2 + y^2 + xy - x - y = 0$.

First we derive the eigenvalues and eigenvectors of $\tilde{U}_X(k)$ and $\tilde{U}_Y(k)$ via two theorems. They are defined as follows:

Theorem III.1. Consider $\tilde{U}_X(k)$ as defined in Eq. (7). Then the set of eigenpairs $(\lambda_j(k), v_j(k))$ of $\tilde{U}_X(k)$ are

$$\lambda_j = e^{i\omega_j(k)},$$

$$|v_j(k)\rangle = \frac{1}{\|f_j(\omega(k))\|} \left[\frac{y + \lambda_j(1-x-y)}{(1-x-y)} + \lambda_j ye^{-ik}, 1, \frac{(1-x-y) + \lambda_j y}{y + \lambda_j(1-x-y)e^{ik}} \right]^T,$$

where $\omega_1(k) = 0$, $\omega_2(k) = -\omega_3(k) = \omega(k)$ with $\cos \omega(k) = x \cos k - (1-x)/2$ and

$$\|f_j(\omega(k))\|^2 = \frac{1+x-2x \cos \omega(k)}{1+x-2x \cos [\omega(k)-k]} + 1 + \frac{1+x-2x \cos \omega(k)}{1+x-2x \cos [\omega(k)+k]},$$

for $j = \{1, 2, 3\}$.

Proof. Note that the characteristic polynomial of $\tilde{U}_X(k)$ is $\kappa_X(\lambda) = \lambda^3 - (2 \cos k + 1)x\lambda^2 + (2 \cos k + 1)x\lambda - 1$. Thus the eigenvalues and the corresponding eigenvectors can be obtained by simple algebraic computations. ■

Let us take $|\Psi(k, 0)\rangle = [\alpha, \beta, \gamma]^T \in \mathbb{C}^3$, where $|\alpha|^2 + |\beta|^2 + |\gamma|^2 = 1$. From Eq. (5),

we have

$$\begin{aligned}
 |\psi(m, t)\rangle &= \sum_{j=1}^3 \frac{1}{2\pi} \int_{-\pi}^{\pi} e^{i[-km+w_j(k)t]} \langle v_j(k) | \Psi(k, 0) \rangle |v_j(k)\rangle dk \\
 &= \sum_{j=1}^3 [\psi_j(m, t, 1, \alpha, \beta, \gamma), \psi_j(m, t, 2, \alpha, \beta, \gamma), \\
 &\quad \psi_j(m, t, 3, \alpha, \beta, \gamma)]^T, \tag{8}
 \end{aligned}$$

where

$$\begin{aligned}
 \psi_j(m, t, l, \alpha, \beta, \gamma) &= \frac{1}{2\pi} \int_{-\pi}^{\pi} e^{i[-km+w_j(k)t]} \langle v_j(k) | \Psi(k, 0) \rangle \langle l | v_j(k) \rangle,
 \end{aligned}$$

and $\{|l| |l = 1, 2, 3\}$ is the canonical basis of \mathbb{C}^3 .

Clearly, $\psi_l(m, t) = \sum_{j=1}^3 \psi_j(m, t, l, \alpha, \beta, \gamma)$, for $l = 1, 2, 3$ and hence

$$P(m, t) = \sum_{l \in \{L, S, R\}} |\psi_l(m, t)|^2 = \sum_{l=1}^3 \sum_{j=1}^3 |\psi_j(m, t, l, \alpha, \beta, \gamma)|^2.$$

Let us denote the probability of finding a particle at node m after time steps t with chirality l by $P(m, t, l)$, then $P(m, t, l) = |\psi_l(m, t)|^2$, where $l = 1, 2, 3$.

Now we state the long-time limit theorem of the DTQWs with coin operators from \mathcal{X} at vertex position m on the line as follows: To derive these theorems, we make use of the well-known Riemann-Lebesgue Lemma [50], which is stated as follows:

Theorem III.2 (Riemann-Lebesgue Lemma). Let f be an integrable real valued function on $[0, 2\pi]$. Then $\lim_{n \rightarrow \infty} \int_0^{2\pi} f(x) \cos(nx) dx = 0$ and $\lim_{n \rightarrow \infty} \int_0^{2\pi} f(x) \sin(nx) dx = 0$.

We prove the following theorem which finds the asymptotic value of the probability measure for finding the particle as $t \rightarrow \infty$ for discrete-time quantum walks using coin operators $C \in \mathcal{X}$.

Theorem III.3. Let $C \in \mathcal{X}$ be not a permutation matrix i.e., $x \neq 0, 1$ and $\Psi(k, 0) = [\alpha, \beta, \gamma]^T$ be the initial state of the

walker. Then for $m \in \mathbb{Z}$

$$\begin{aligned}
 \lim_{t \rightarrow \infty} P(m, t) &\sim \frac{1}{3(1-x)(x+3)} \{ |Av^{|m|} + Bv^{|-m+1}| \}^2 \\
 &\quad + |\alpha(1-x-y)v^{|m|} + \alpha y v^{|m+1}| + \beta(1+x)v^{|m|} \\
 &\quad - \beta x v^{|-m+1}| - \beta x v^{|m+1}| + \gamma(1-x-y)v^{|-m+1}| \\
 &\quad + \gamma y v^{|m|} \}^2 + |Av^{|m+1}| + Bv^{|m|} \}^2,
 \end{aligned}$$

where

$$v = -\frac{(x-3) + \sqrt{3(1-x)(x+3)}}{2x},$$

$$A = \alpha(1-x) + \beta(1-x-y),$$

$$B = \gamma(1-x) + \beta y.$$

If $C \in \mathcal{X}$ are permutation matrices and $|\Psi(k, 0)\rangle = [\alpha, \beta, \gamma]^T$ is the initial state of the walker, then for $m \in \mathbb{Z}$,

$$\begin{aligned}
 \lim_{t \rightarrow \infty} P(m, t) &\sim \begin{cases} |\beta|^2 & \text{if } m = 0, C = I \\ \frac{1}{3}(|\alpha|^2 + 2|\beta + \gamma|^2) & \text{if } m = 0, C = P_{(123)} \\ \frac{1}{3}|\beta + \gamma|^2 & \text{if } m = -1, C = P_{(123)} \\ \frac{2}{3}|\alpha|^2 & \text{if } m = 1, C = P_{(123)} \\ \frac{1}{3}(|\gamma|^2 + 2|\alpha + \beta|^2) & \text{if } m = 0, C = P_{(132)} \\ \frac{2}{3}|\gamma|^2 & \text{if } m = -1, C = P_{(132)} \\ \frac{1}{3}|\alpha + \beta|^2 & \text{if } m = 1, C = P_{(132)} \\ 0, & \text{otherwise.} \end{cases}
 \end{aligned}$$

Proof. The asymptotic nature of the amplitude vector can be derived by Riemann-Lebesgue Lemma for infinite time steps (see Appendix A for the details) so that

$$\begin{aligned}
 |\psi(m, t)\rangle &= \sum_{j=1}^3 \frac{1}{2\pi} \int_{-\pi}^{\pi} e^{i[-km+w_j(k)t]} \langle v_j(k) | \Psi(k, 0) \rangle |v_j(k)\rangle dk \\
 &\sim \frac{1}{2\pi} \int_{-\pi}^{\pi} e^{-ikm} \langle v_1(k) | \Psi(k, 0) \rangle |v_1(k)\rangle dk \text{ (for } t \rightarrow \infty).
 \end{aligned}$$

Thus,

$$\begin{aligned}
 |\psi(m, t)\rangle &\sim \frac{1}{2\pi} \int_{-\pi}^{\pi} \frac{1}{\|f_1(\omega(k))\|^2} \left[\frac{1-x}{(1-x-y) + ye^{-ik}}, 1, \frac{1-x}{y + (1-x-y)e^{ik}} \right]^T \\
 &\quad \times \left[\alpha \frac{1-x}{(1-x-y) + ye^{ik}} + \beta + \gamma \frac{1-x}{y + (1-x-y)e^{-ik}} \right] e^{-ikm} dk \text{ (for } t \rightarrow \infty) \\
 &= [\psi_1(m, t, 1, \alpha, \beta, \gamma), \psi_1(m, t, 2, \alpha, \beta, \gamma), \psi_1(m, t, 3, \alpha, \beta, \gamma)]^T.
 \end{aligned}$$

By Theorem III.1 we have

$$\frac{1}{\|f_1(\omega(k))\|^2} = \frac{1+x-2x \cos k}{3-x-2x \cos k},$$

for $\lambda_1 = e^{i\omega_1(k)} = 1$ and hence the coefficient of α in the expression of $\psi_1(m, t, 1, \alpha, \beta, \gamma)$ is equal to

$$\frac{1}{2\pi} \int_{-\pi}^{\pi} \frac{(1-x)^2}{(1-x-y+ye^{-ik})(1-x-y+ye^{ik})} \left(\frac{1+x-2x \cos k}{3-x-2x \cos k} \right) e^{-ikm} dk.$$

Whenever $x \notin \{0, 1\}$, i.e., $C \in \mathcal{X}$ is not a permutation matrix, the above expression simplifies to

$$\frac{1}{2\pi} \int_{-\pi}^{\pi} \frac{(1-x)}{3-x-2x \cos k} e^{-ikm} dk = \frac{1}{2\pi} \int_{-\pi}^{\pi} \frac{(1-x) \cos km}{3-x-2x \cos k} dk = \frac{1}{\sqrt{3(1-x)(x+3)}} (1-x)v^{|m|},$$

where

$$v = -\frac{(x-3) + \sqrt{3(1-x)(x+3)}}{2x}.$$

Similarly, we calculate for the others and come up with the following:

$$\begin{aligned} |\psi(m, t)\rangle \sim & \frac{1}{\sqrt{3(1-x)(x+3)}} [\alpha(1-x)v^{|m|} + \beta(1-x-y)v^{|m|} + \beta\gamma v^{|-m+1|} + \gamma(1-x)v^{|-m+1|}, \\ & \alpha(1-x-y)v^{|m|} + \alpha\gamma v^{|-m-1|} + \beta(1+x)v^{|m|} - x\beta v^{|-m+1|} - x\beta v^{|-m-1|} + \gamma(1-x-y)v^{|-m+1|} + \gamma\gamma v^{|m|}, \\ & \alpha(1-x)v^{|-m-1|} + \beta\gamma v^{|m|} + \beta(1-x-y)v^{|-m-1|} + \gamma(1-x)v^{|m|}]. \end{aligned}$$

Thus the statement of the theorem follows after computing the norm of $\psi(m, t)$. Now let us take C to be the permutation coin. This can be obtained from \mathcal{X} by substituting either $x = 0$ or $x = 1$.

First let $x = 1$, then C is the identity matrix. Clearly the eigenvalues of corresponding $\tilde{U}(k)$ are $e^{ik}, 1, e^{-ik}$. Thus,

$$|\psi(m, t)\rangle \sim \frac{1}{2\pi} \int_{-\pi}^{\pi} \langle 2|\Psi(k, 0)\rangle e^{-ikm} |2\rangle dk \text{ (for } t \rightarrow \infty),$$

where $|2\rangle = [0, 1, 0]^T$. This results $\lim_{t \rightarrow \infty} P(m, t) = |\beta|^2$ for $m = 0$ and $\lim_{t \rightarrow \infty} P(m, t) = 0$ for $m \neq 0$.

Let $x = 0$ then either $y = 0$ or $y = 1$. If $y = 1$ then $C = P_{(123)}$. Correspondingly, the eigenvalues of $\tilde{U}(k)$ are ω, ω^2 , and 1 where $\omega = e^{\frac{2\pi i}{3}}$. In this case,

$$\begin{aligned} |\psi(m, t)\rangle \sim & \frac{1}{2\pi} \int_{-\pi}^{\pi} [\alpha + (\beta + \gamma)e^{ik}, \alpha e^{-ik} + (\beta + \gamma), \\ & \alpha e^{-ik} + (\beta + \gamma)]^T e^{-ikm} dk \text{ (} t \rightarrow \infty). \end{aligned}$$

If $x = 0$ and $y = 0$, then $C = P_{(132)}$. The eigenvalues of $\tilde{U}(k)$ are ω, ω^2 , and 1 where $\omega = e^{\frac{2\pi i}{3}}$. Hence we get

$$\begin{aligned} |\psi(m, t)\rangle \sim & \frac{1}{2\pi} \int_{-\pi}^{\pi} [(\alpha + \beta) + \gamma e^{ik}, (\alpha + \beta) + \gamma e^{ik}, \\ & (\alpha + \beta)e^{-ik} + \gamma]^T e^{-ikm} dk, \end{aligned}$$

setting $t \rightarrow \infty$. This completes the proof. \blacksquare

To corroborate the theoretical findings of Theorem III.3, we plot Fig. 1. We compare the limiting probability of the walker to be at some vertex m of the line, i.e., $\lim_{t \rightarrow \infty} P(m, t)$, obtained in the aforementioned theorems with the actual probability of the walker to be at m after a large but finite number of steps. For Fig. 1, we consider a DTQW starting from origin and using a coin operator from the family $\mathcal{C} \in \mathcal{X}$. In all the figures we observe that the probability of finding the particle is maximum around the origin.

Using the computable expression of $\lim_{t \rightarrow \infty} P(m, t)$ as derived in Theorem III.3, the localization condition for the

DTQWs according to the definition given in Ref. [46] is

$$\begin{aligned} & \left[\frac{1+v^2}{1-v^2} (2|A|^2 + 2|B|^2 + |T_1|^2 + |T_2|^2 + |T_3|^2) + \frac{4v}{1-v^2} \right. \\ & \quad \times [\text{Re}(A\bar{B}) + \text{Re}(T_1\bar{T}_2) + \text{Re}(T_1\bar{T}_3)] \\ & \quad \left. + 2v^2 \frac{3-v^2}{1-v^2} \text{Re}(T_2\bar{T}_3) \right] > 0, \end{aligned}$$

where $T_1 = \alpha(1-x-y) + \beta(1+x) + \gamma\gamma$, $T_2 = \alpha\gamma - \beta x$, $T_3 = -\beta x + \gamma(1-x-y)$. Note that $-5 + 2\sqrt{6} \leq v < 1$ when $x \neq 0, 1$ so that $1 - v^2 \neq 0$. This follows from the derivation in Appendix B.

Let us now choose the initial coin state $\alpha = \frac{1}{\sqrt{3}} = \beta = \gamma$. Then from Theorem III.3,

$$\begin{aligned} \lim_{t \rightarrow \infty} P(0, t) = & \frac{1}{3(1-x)(x+3)} \left[|A + Bv|^2 \right. \\ & \left. + \frac{1}{3} |2 + v(1-3x)|^2 + |Av + B|^2 \right]. \end{aligned}$$

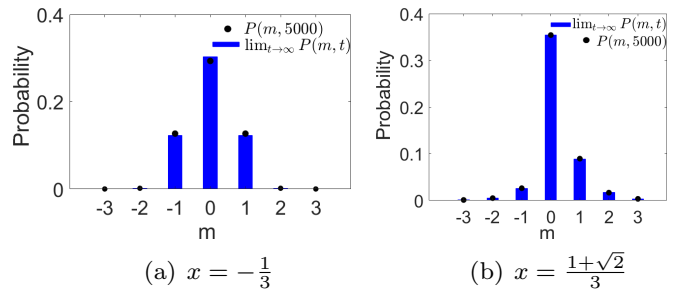


FIG. 1. Panels (a) and (b) compare the probability distribution $P(m, t)$ at time $t = 5000$ (black points) and the limit measure $\lim_{t \rightarrow \infty} P(m, t)$ (blue bars) when the underlying coin operators are from the collection \mathcal{X} and correspond to $x = -\frac{1}{3}$ and $x = \frac{1+\sqrt{2}}{3}$, respectively; with initial coin state $[\frac{1}{\sqrt{3}}, \frac{1}{\sqrt{3}}, \frac{1}{\sqrt{3}}]^T$. We get $P(0, 5000) = 0.2934$, $\lim_{t \rightarrow \infty} P(0, t) = 0.3031$ for panel (a) and $P(0, 5000) = 0.3542$, $\lim_{t \rightarrow \infty} P(0, t) = 0.3548$ for panel (b).

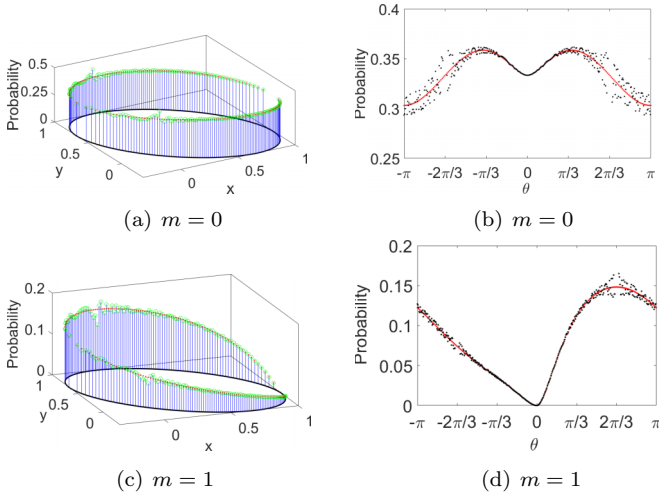


FIG. 2. The initial coin state is taken as $[\frac{1}{\sqrt{3}}, \frac{1}{\sqrt{3}}, \frac{1}{\sqrt{3}}]^T$ for all the walks. In panels (a) and (c), we compare the values $P(m, 5000)$ (green points) and $\lim_{t \rightarrow \infty} P(m, t)$ (red point) for the walker's positions at the origin i.e., $m = 0$ and $m = 1$, respectively; with coin operators correspond to different values of (x, y) changes along $x^2 + y^2 - x - y + xy = 0$, $-\frac{1}{3} \leq x, y \leq 1$. Besides, we draw the probabilities $P(m, 5000)$ (black points) and $\lim_{t \rightarrow \infty} P(m, t)$ (red points) due to the change in $\theta \in [-\pi, \pi]$, $\theta \neq 0, \frac{2\pi}{3}, -\frac{2\pi}{3}$, where $x = (1 + 2 \cos \theta)/3$, for positions $m = 0$ and $m = 1$, given in panels (b) and (d), respectively.

$$\mathcal{X}_\theta = \left\{ \begin{bmatrix} \frac{2 \cos \theta + 1}{3} & \frac{(1 - \cos \theta)}{3} + \frac{1}{\sqrt{3}} \sin \theta & \frac{(1 - \cos \theta)}{3} - \frac{1}{\sqrt{3}} \sin \theta \\ \frac{(1 - \cos \theta)}{3} - \frac{1}{\sqrt{3}} \sin \theta & \frac{2 \cos \theta + 1}{3} & \frac{(1 - \cos \theta)}{3} + \frac{1}{\sqrt{3}} \sin \theta \\ \frac{(1 - \cos \theta)}{3} + \frac{1}{\sqrt{3}} \sin \theta & \frac{(1 - \cos \theta)}{3} - \frac{1}{\sqrt{3}} \sin \theta & \frac{2 \cos \theta + 1}{3} \end{bmatrix} : -\pi \leq \theta \leq \pi \right\}.$$

It is clear from the parametrization that if $A(\theta) \in \mathcal{X}_\theta$ then $[A(\theta)]^{-1} = A(-\theta)$. In Fig. 2, we compare the long-time-limit probabilities with the probability at a large but finite time, at two different positions $m = 0, 1$, across the range of coin parameters from \mathcal{X} . In each case we set $\alpha = \beta = \gamma = \frac{1}{\sqrt{3}}$. The diagrams in Figs. 2(a) and 2(c) show the change in probability values along the ellipse $x^2 + y^2 - x - y + xy = 0$, $-\frac{1}{3} \leq x, y \leq 1$; the diagrams in Figs. 2(b) and 2(d) are plotted recording the changes in parameter θ for $[-\pi, \pi]$. We see that the probabilities take the relative minimum value around $(x, y) = (1, 0)$ or consequently around $\theta = 0$. A relative maximum values for both the probability at $t = 5000$ and limit

Since $2 + \nu(1 - 3x) \neq 0$ for $x \neq 0, 1$, we get $\lim_{t \rightarrow \infty} P(0, t) > 0$. Correspondingly, the walks with coins from \mathcal{X} , $x \neq 0, 1$ show localization at $m = 0$. Figure 2 supports this fact.

In fact we establish the following corollary from Theorem III.3 regarding the initial states that lead zero value to the limiting probabilities.

Corollary III.4. Let $C \in \mathcal{X}$ and $x \neq 0, 1$. Then $\lim_{t \rightarrow \infty} P(0, t) = 0$ if and only if $|\Psi(k, 0)\rangle = \frac{1}{N}[(1 - x - y), -(1 - x), y]^T$, $N = [(1 - x - y)^2 + (1 - x)^2 + y^2]^{1/2}$.

Proof. The limiting probability takes zero value for the walks under consideration, whenever $A = B = 0$ and $x \neq 0, 1$. Hence the corresponding initial state reads $|\Psi(k, 0)\rangle := |\Psi_{\mathcal{X}}\rangle = \frac{1}{N}[(1 - x - y), -(1 - x), y]^T$, for which $\lim_{t \rightarrow \infty} P(0, t)$ of the walks with coins from \mathcal{X} , $x \neq 0, 1$ vanishes. ■

Indeed, it can be checked that $|\Psi_{\mathcal{X}}\rangle$ is orthogonal to the eigenvector $|v_1(k)\rangle$ given in Theorem III.1 corresponds to the eigenvalue 1.

Now we redefine the set of matrices in \mathcal{X} that can be represented by a single parameter θ . To this end, for $-\pi \leq \theta \leq \pi$, setting

$$(x, y) = \left(\frac{1 + 2 \cos \theta}{3}, \frac{1 - \cos \theta}{3} + \frac{1}{\sqrt{3}} \sin \theta \right),$$

yields one-parameter representation for the matrices in \mathcal{X} in terms of the parameter θ [28]. We call this matrix class as \mathcal{X}_θ , where

measure appear for $(x, y) = (0, 1)$ and $\theta = \frac{2\pi}{3}$ in Figs. 2(c) and 2(d), respectively. Besides, it is easy to see from Fig. 2 that $\lim_{t \rightarrow \infty} P(m, t)$ at the initial position $m = 0$ is equal for the coin operators $A(\theta)$ and its inverse $[A(-\theta)]$.

B. Coins from \mathcal{Y}

In what follows, we provide a limit theorem for the proposed walks with coin operators from \mathcal{Y} . We perform a similar analysis as above. For $C \in \mathcal{Y}$, $k \in (-\pi, \pi]$, $\tilde{U}_{\mathcal{Y}}(k) = D(k)C$ is given by

$$\tilde{U}_{\mathcal{Y}}(k) = \begin{bmatrix} xe^{ik} & ye^{ik} & (-1 - x - y)e^{ik} \\ -1 - x - y & x & y \\ ye^{-ik} & (-1 - x - y)e^{-ik} & xe^{-ik} \end{bmatrix}, \quad (9)$$

where $x^2 + y^2 + xy + x + y = 0$.

The following theorem provides computable expressions for eigenvalues and eigenvectors of $\tilde{U}_{\mathcal{Y}}(k)$:

Theorem III.5. Consider $\tilde{U}_{\mathcal{Y}}(k)$ in Eq. (9). Then the set of eigenpairs $(\lambda_j(k), v_j(k))$ of $\tilde{U}_{\mathcal{Y}}(k)$ are

$$\lambda_j = e^{i\omega_j(k)}, \quad |v_j(k)\rangle = \frac{1}{\|f_j(\omega(k))\|} \left[\frac{-y + \lambda_j(1+x+y)}{(1+x+y) - \lambda_j y e^{-ik}}, 1, \frac{(1+x+y) - \lambda_j y}{-y + \lambda_j(1+x+y)e^{ik}} \right]^T,$$

where $\omega_1(k) = \pi, \omega_2(k) = -\omega_3(k) = \omega(k)$ with $\cos \omega(k) = -x \cos k - \frac{(1+x)}{2}$ and

$$\|f_j(\omega(k))\|^2 = \frac{1-x-2x \cos \omega(k)}{1-x-2x \cos [\omega(k)-k]} + 1 + \frac{1-x-2x \cos \omega(k)}{1-x-2x \cos [\omega(k)+k]},$$

for $\{j = 1, 2, 3\}$.

Proof. Note that the characteristic polynomial of $\tilde{U}_{\mathcal{Y}}(k)$ is $\kappa_{\mathcal{Y}}(\lambda) = \lambda^3 - (2 \cos k + 1)x\lambda^2 - (2 \cos k + 1)x\lambda + 1$. Hence the desired results follow after simple algebraic calculations. ■

The next theorem concerns the asymptotic value of the probability measure for finding the particle to be at any vertex m , as $t \rightarrow \infty$, for a DTQW using coin operators $C \in \mathcal{Y}$.

Theorem III.6. Let $C \in \mathcal{Y}$ be not a permutation matrix, i.e., $x \neq 0, -1$ and $\Psi(k, 0) = [\alpha, \beta, \gamma]^T$ be the initial state of the walker, then for $m \in \mathbb{Z}$ we get

$$\lim_{t \rightarrow \infty} P(m, t) \sim \frac{1}{3(1+x)(3-x)} \{ |D\mu^{|m|} + E\mu^{|-m+1}|^2 + |\alpha(1+x+y)\mu^{|m|} - \alpha y \mu^{|m+1}| + \beta(1-x)\mu^{|m|} + \beta x(\mu^{|-m+1}| + \mu^{|m+1}|) + \gamma(1+x+y)\mu^{|-m+1}| - \gamma y \mu^{|m|}|^2 + |D\mu^{|m+1}| + E\mu^{|m|}|^2 \},$$

where

$$\mu = \frac{-(x+3) + \sqrt{3(1+x)(3-x)}}{2x},$$

$$D = \alpha(1+x) + \beta(1+x+y),$$

$$E = \gamma(1+x) - \beta y.$$

If $C \in \mathcal{Y}$ are permutation matrices and $\Psi(k, 0) = [\alpha, \beta, \gamma]^T$ is the initial state of the walker, then for $m \in \mathbb{Z}$ we have the following:

$$\lim_{t \rightarrow \infty} P(m, t) \sim \begin{cases} |\beta|^2 & \text{if } m = 0, C = I \\ \frac{1}{3}(|\alpha|^2 + 2|\beta + \gamma|^2) & \text{if } m = 0, C = -P_{(213)} \\ \frac{1}{3}|\beta + \gamma|^2 & \text{if } m = -1, C = P_{(123)} \\ \frac{2}{3}|\alpha|^2 & \text{if } m = 1, C = P_{(123)} \\ \frac{1}{3}(|\gamma|^2 + 2|\alpha + \beta|^2) & \text{if } m = 0, C = P_{(132)} \\ \frac{2}{3}|\gamma|^2 & \text{if } m = -1, C = P_{(132)} \\ \frac{1}{3}|\alpha + \beta|^2 & \text{if } m = 1, C = P_{(132)} \\ 0, & \text{otherwise.} \end{cases}$$

Proof. The proof follows adapting a similar approach as in Theorem III.3. ■

In Fig. 3, we compare the numerical values of $P(m, t), t = 10\,000$ and the limiting value of the probability measure fixing the same initial state, when the initial position of the walker is the origin; that is, $m = 0$ for two different coins from \mathcal{Y} . The figures support the localization phenomena.

The walks with coin operators from \mathcal{Y} localize according to Ref. [46] if

$$\begin{aligned} & \left[\frac{1 + \mu^2}{1 - \mu^2} (2|D|^2 + 2|E|^2 + |S_1|^2 + |S_2|^2 + |S_3|^2) \right. \\ & + \frac{4\mu}{1 - \mu^2} [\text{Re}(DE) + \text{Re}(S_1\bar{S}_2) + \text{Re}(S_1\bar{S}_3)] \\ & \left. + 2\mu^2 \frac{3 - \mu^2}{1 - \mu^2} \text{Re}(S_2\bar{S}_3) \right] > 0, \end{aligned}$$

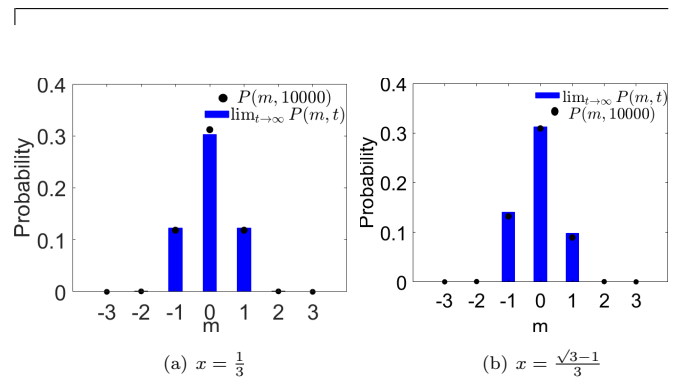


FIG. 3. Panels (a) and (b) compare $P(m, t)$ for $t = 10\,000$ (black points) and $\lim_{t \rightarrow \infty} P(m, t)$, (blue bars) when the underlying coin operators are from \mathcal{Y} correspond to $x = \frac{1}{3}$ and $x = \frac{\sqrt{3}-1}{3}$, respectively; with initial coin state $[\frac{1}{\sqrt{3}}, \frac{1}{\sqrt{3}}, \frac{1}{\sqrt{3}}]^T$. We get $P(0, 10\,000) = 0.3120, \lim_{t \rightarrow \infty} P(0, t) = 0.3031$ for panel (a) and $P(0, 10\,000) = 0.3092, \lim_{t \rightarrow \infty} P(0, t) = 0.3123$ for panel (b).

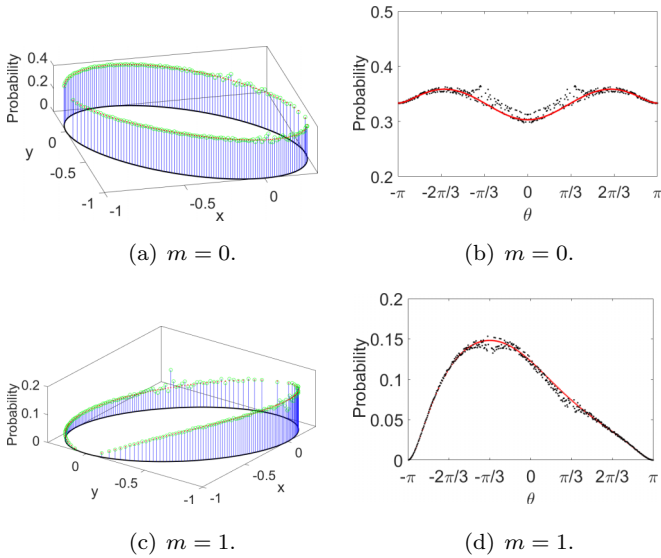


FIG. 4. Here the coin operators under consideration are chosen from \mathcal{Y} , $x \neq -1, 0$ and the initial coin state is $[\frac{1}{\sqrt{3}}, \frac{1}{\sqrt{3}}, \frac{1}{\sqrt{3}}]^T$ in all the cases. In panels (a) and (c) we compare the values for probability at $t = 10000$ (green points) and limit probability measure (red point) for the walker's positions at $m = 0$ and $m = 1$, respectively, with different coin operators. Also, we draw the probabilities $P(m, 10000)$ (black points) and $\lim_{t \rightarrow \infty} P(m, t)$ (red points) for different values of $\theta \in [-\pi, \pi]$, $\theta \neq \pi, -\pi, \frac{\pi}{3}, -\frac{\pi}{3}$,

where $S_1 = \alpha(1+x+y) + \beta(1-x) - \gamma y$, $S_2 = -\alpha y + \beta x$, $S_3 = \beta x + \gamma(1+x+y)$ and $-5 + 2\sqrt{6} \leq \mu < 1$, $\mu^2 < 1$. See Appendix B for the derivation.

$$\mathcal{Y}_\theta = \left\{ \begin{bmatrix} \frac{2 \cos \theta - 1}{3} & -\frac{(1 + \cos \theta)}{3} + \frac{1}{\sqrt{3}} \sin \theta & -\frac{(1 + \cos \theta)}{3} - \frac{1}{\sqrt{3}} \sin \theta \\ -\frac{(1 + \cos \theta)}{3} - \frac{1}{\sqrt{3}} \sin \theta & \frac{2 \cos \theta - 1}{3} & -\frac{(1 + \cos \theta)}{3} + \frac{1}{\sqrt{3}} \sin \theta \\ -\frac{(1 + \cos \theta)}{3} + \frac{1}{\sqrt{3}} \sin \theta & -\frac{(1 + \cos \theta)}{3} - \frac{1}{\sqrt{3}} \sin \theta & \frac{2 \cos \theta - 1}{3} \end{bmatrix} : -\pi \leq \theta \leq \pi \right\}.$$

Note that, if $\theta \in \{\pi, -\pi, \frac{\pi}{3}, -\frac{\pi}{3}\}$, we obtain the negative of the permutation matrices in \mathcal{Y}_θ . Also, if $A(\theta) \in \mathcal{Y}_\theta$ then $[A(\theta)]^{-1} = A(-\theta)$. In Fig. 4, we see the limiting values of the probability measure for the walks where the coin parameter (x, y) changes along the ellipse $x^2 + y^2 + x + y + xy = 0$, $-1 \leq x, y \leq \frac{1}{3}$; or the coin parameter $\theta \in [-\pi, \pi]$. In Figs. 4(b) and 4(d), the probabilities take the relative minimum and maximum values are around $\theta = 0$ and $\theta = -\frac{\pi}{3}$, respectively. In Figs. 4(c) and 4(d), the probability values are getting near to zero in the neighborhood of $(x, y) = (-1, 0)$ and $\theta = \pm\pi$, respectively. Finally, observe from Fig. 4 that $\lim_{t \rightarrow \infty} P(m, t)$ at the initial position $m = 0$ is equal for the coin operator $A(\theta)$ and its inverse $[A(-\theta)]$.

IV. PEAK VELOCITIES OF THE WALKS

In Sec. III we established that the discrete-time quantum walks with coin operators from the family \mathcal{X}_θ and \mathcal{Y}_θ localize.

Also, from Theorem III.5, we write

$$\lim_{t \rightarrow \infty} P(0, t) = \frac{1}{3(1+x)(3-x)} \left[|D + E\mu|^2 + \frac{1}{3} |2 + \mu(1+3x)|^2 + |D\mu + E|^2 \right].$$

Since $2 + \mu(1+3x) \neq 0$ for $x \neq 0, -1$, we get $\lim_{t \rightarrow \infty} P(0, t) > 0$ and we say the walks with coins from \mathcal{Y} , $x \neq 0, -1$ show localization at $m = 0$. To account for this fact we have Fig. 4. In fact, we establish the following corollary from Theorem III.6 regarding the initial states that lead to zero value for the limiting probabilities.

Corollary III.7. Let $C \in \mathcal{Y}$ and $x \neq 0, -1$. Then $\lim_{t \rightarrow \infty} P(0, t) = 0$ if and only if $|\Psi(k, 0)\rangle = \frac{1}{N} [-(1+x+y), (1+x), y]^T$, $N = [(1+x+y)^2 + (1+x)^2 + y^2]^{1/2}$.

Proof. We get $\lim_{t \rightarrow \infty} P(0, t) = 0$ whenever $D = E = 0$ and $x \neq 0, -1$. Therefore, the corresponding initial state is $|\Psi(k, 0)\rangle := |\Psi_{\mathcal{Y}}\rangle = \frac{1}{N} [-(1+x+y), (1+x), y]^T$, for which the limiting probability at $m = 0$ of the walks with coins from \mathcal{Y} , $x \neq 0, -1$ vanishes. ■

Indeed, it can be checked that $|\Psi_{\mathcal{Y}}\rangle$ is orthogonal to the eigenvector $|v_1(k)\rangle$ given in Theorem III.5 and corresponds to the eigenvalue -1 .

Now we redefine the set of matrices in \mathcal{Y} can be represented by a single parameter θ . To this end, for $-\pi \leq \theta \leq \pi$, for the set of matrices in \mathcal{Y} , setting

$$(x, y) = \left(\frac{2 \cos \theta - 1}{3}, -\frac{1 + \cos \theta}{3} + \frac{1}{\sqrt{3}} \sin \theta \right)$$

yields one-parameter representation for the matrices in \mathcal{X} and \mathcal{Y} in terms of the parameter θ [28]. We call this matrix class \mathcal{Y}_θ , where

This was done by demonstrating that there exists a nonvanishing probability for the quantum walk to remain at a vertex even as the time steps of the walk approach infinity. In this section, we discuss the localization phenomena of the walks from a different perspective.

In Ref. [31], the authors establish a relationship between the choice of the coin parameters and the peak velocity with which the underlying quantum walk wave function spreads. The authors demonstrate this by considering a generalized Grover operator as coin, obtained by modifying its eigenvalues and eigenvectors. Peak velocities control the limit distribution and in turn influences localization.

Here at first, we determine the peak velocities of the probability distribution of the walker's position when the coin operators are from \mathcal{X}_θ and \mathcal{Y}_θ . This allows us to provide a new family of parametrized coin operators \mathcal{X}_θ , outside those in Ref. [31], which preserves the localization of the Grover walk. We describe how the coin parameter θ relates the spreading of the walks through the line.

Recall that, from Eq. (8), we have

$$|\psi(m, t)\rangle = \sum_{j=1}^3 \frac{1}{2\pi} \int_{-\pi}^{\pi} e^{i[-km/t + \omega_j(k)t]} \langle v_j(k) | \Psi(k, 0) \rangle \times |v_j(k)\rangle dk. \tag{10}$$

Now to determine the behavior of $|\psi(m, t)\rangle$ as $t \rightarrow \infty$, we employ the idea given in Ref. [31] by using the method of stationary phase approximation (SPA) [51].

In general, the SPA states that, for a propagating wave packet, the contributions of the fast oscillating phases average out and only the amplitudes corresponding to the stationary phases contribute significantly to the overall wave function of the wave packet. The propagation of the wave function corresponding to a quantum walk on an infinite line with periodic boundary conditions can be modeled using the theory of the SPA.

Consider the phase $\bar{\omega}_j(k) = \omega_j(k) - mk/t$ from Eq. (10). Now, the rate of decay is given by the order of the stationary points of the phase $\bar{\omega}_j(k)$. By solving the equation $\frac{d^2}{dk^2} \bar{\omega}_j(k) = 0$, we find the stationary points corresponding to the maximum value of $\frac{d}{dk} \bar{\omega}_j(k)$. If k_0 is the solution of the second-order derivative then by equating the first-order equation $\frac{d}{dk} \bar{\omega}_j(k) = \frac{d}{dk} \omega_j(k) - m/t$ with zero we get the position of the peak after time t as $m = \frac{d}{dk} \omega_j(k)|_{k_0} t$, whereas the peaks in the probability distribution curve propagates with the maximal group velocity $\frac{d}{dk} \omega_j(k)|_{k_0}$. Here we recall that the group velocity of the propagating wave function corresponding to the quantum walk is simply $\frac{d}{dk} \omega_j(k)$, where k and $\omega_j(k)$ are the wave number and angular frequency, respectively [41].

Next we obtain peak velocities for the wave function corresponding to a discrete-time quantum walk on a line with generalized coin operators chosen from the sets \mathcal{X}_θ and \mathcal{Y}_θ .

A. With coin operators $C \in \mathcal{X}_\theta$

First we consider the walk with coins from \mathcal{X} . Now for $x = (1 + 2 \cos \theta)/3$, by Theorem III.1 the eigenvalues of $\tilde{U}_{\mathcal{X}}(k)$ are $\lambda_j = e^{i\omega_j(k)}$, $j = 1, 2, 3$, where $\omega_1(k) = 0$, $\omega_2(k) = -\omega_3(k) = \omega(k)$ with $\cos \omega(k) = -\frac{1}{3}(1 - \cos k) + \frac{\cos \theta}{3}(1 + 2 \cos k)$.

Since $\omega_1(k)$ is independent of the wave number k , the localization effect of the quantum walks using \mathcal{X}_θ as the coin operator is preserved as that of the Grover walk [21,23]. Indeed, the existence of constant eigenvalues of the time evolution operator and the localization are equivalent for DTQWs on infinite lattice under cyclic boundary conditions [47].

We shall now determine the peak velocities using the coin operators from \mathcal{X}_θ for $\theta = 0, \frac{2\pi}{3}, -\frac{2\pi}{3}$, which are permutation matrices. For $\theta = 0$, \mathcal{X}_θ becomes the identity matrix. Therefore, $\omega_2(k) = \pm k$ and $\omega_3(k) = \pm k$, consequently the right- and left-going peak velocities are

$$v_R = \frac{d}{dk} \omega_3(k) = -1, \quad v_L = \frac{d}{dk} \omega_2(k) = 1,$$

whereas $\frac{d^2}{dk^2} \omega_2(k) = \frac{d^2}{dk^2} \omega_3(k) = 0$.

Similarly, if $\theta = \frac{2\pi}{3}$ or $\theta = -\frac{2\pi}{3}$ we get permutation matrices $P_{(123)} \in \mathcal{X}_\theta$ or $P_{(132)} \in \mathcal{X}_\theta$ respectively. For both the cases the eigenvalues $\omega_2(k) = \pm \frac{2\pi}{3}$ and $\omega_3(k) = \pm \frac{2\pi}{3}$ and hence the corresponding peak velocities are 0. If θ equals to $-\pi$ or π , accordingly the coin operator is the Grover matrix, the right and left peak velocities are $\frac{1}{\sqrt{3}}$ and $-\frac{1}{\sqrt{3}}$, respectively [31].

From now onward we consider coins from the family \mathcal{X}_θ except the Grover and permutation matrices, i.e., $(1 + 2 \cos \theta) \neq 0, 3, -1$. Now, to find the peak velocities we determine for which values of k the second derivatives of $\omega_2(k)$ and $\omega_3(k)$ vanish. Thus,

$$\frac{d^2 \omega_2(k)}{dk^2} = \frac{\cos k(1 + 2 \cos \theta)}{\{9 - [-1 + \cos k + \cos \theta(1 + 2 \cos k)]^2\}^{\frac{1}{2}} \frac{\sin^2 k(1 + 2 \cos k)^2[-1 + \cos k + \cos \theta(1 + 2 \cos k)]}{\{9 - [-1 + \cos k + \cos \theta(1 + 2 \cos k)]^2\}^{\frac{3}{2}}}$$

vanishes for

$$k_0^1 = \pi - \arccos \left(\frac{5 \cos \theta + 7 - 3\sqrt{\cos^2 \theta + 6 \cos \theta + 5}}{2(2 \cos \theta + 1)} \right)$$

and

$$k_0^2 = \pi - \arccos \left(\frac{5 \cos \theta + 7 + 3\sqrt{\cos^2 \theta + 6 \cos \theta + 5}}{2(2 \cos \theta + 1)} \right).$$

Then we determine the group velocities given by

$$\frac{d\omega_2(k)}{dk} = -\frac{d\omega_3(k)}{dk} = \frac{\frac{1}{3} \sin k(1 + 2 \cos \theta)}{\sqrt{1 - [-\frac{1}{3}(1 - \cos k) + \frac{1}{3} \cos \theta(1 + 2 \cos k)]^2}}$$

at the stationary points k_1^0 and k_2^0 . Hence the velocities of the right- and left-going probability peaks v_R and v_L are given by

$$\begin{aligned}
 v_L^{(1)}(\theta) &= \left. \frac{d\omega_2(k)}{dk} \right|_{k=k_1^0} \\
 &= \begin{cases} \frac{1}{3} \sqrt{\frac{9\sqrt{\cos^2\theta+6\cos\theta+5-(15\cos\theta+21)}}{\sqrt{\cos^2\theta+6\cos\theta+5-(\cos\theta+3)}}} & \text{if } -\frac{2\pi}{3} < \theta < -\frac{\pi}{3} \\ -\frac{1}{3} \sqrt{\frac{9\sqrt{\cos^2\theta+6\cos\theta+5-(15\cos\theta+21)}}{\sqrt{\cos^2\theta+6\cos\theta+5-(\cos\theta+3)}}} & \text{if } -\pi < \theta < -\frac{2\pi}{3}, \frac{2\pi}{3} < \theta < \pi, \end{cases} \\
 v_R^{(1)}(\theta) &= \left. \frac{d\omega_3(k)}{dk} \right|_{k=k_1^0} = -v_L^{(1)}(\theta), \\
 v_L^{(2)}(\theta) &= \left. \frac{d\omega_2(k)}{dk} \right|_{k=k_2^0} \\
 &= \begin{cases} \frac{1}{3} \sqrt{\frac{9\sqrt{\cos^2\theta+6\cos\theta+5+(15\cos\theta+21)}}{\sqrt{\cos^2\theta+6\cos\theta+5+(\cos\theta+3)}}} & \text{if } -\frac{2\pi}{3} < \theta < -\frac{\pi}{3} \\ -\frac{1}{3} \sqrt{\frac{9\sqrt{\cos^2\theta+6\cos\theta+5+(15\cos\theta+21)}}{\sqrt{\cos^2\theta+6\cos\theta+5+(\cos\theta+3)}}} & \text{if } -\pi < \theta < -\frac{2\pi}{3}, \frac{2\pi}{3} < \theta < \pi, \end{cases} \\
 v_R^{(2)}(\theta) &= \left. \frac{d\omega_3(k)}{dk} \right|_{k=k_2^0} = -v_L^{(2)}(\theta),
 \end{aligned}$$

where $(1 + 2 \cos \theta) \neq 0, 3, -1$. It is worthy to mention that $v_S^{(1)}(\theta) = v_S^{(2)}(\theta) = 0$.

Here we mention that $v_R(\theta)$ and $v_L(\theta)$ do not keep the same sign for all the coin parametric values θ through the interval $[\pi, \pi]$, in contrast with the study in Ref. [31]. Henceforth, in order to get rid of the conflict with the names ‘‘velocity of the right-going peaks’’ and ‘‘velocity of the left-going peaks,’’ which are generally used in case of positive and negative quantities, we emphasize that we represent $v_R(\theta)$ and $v_L(\theta)$, respectively, by the expressions $\left. \frac{d\omega_2(k)}{dk} \right|_{k=k^0}$ and $\left. \frac{d\omega_3(k)}{dk} \right|_{k=k^0}$ only, not in the sense of sign.

We plot the functions $v_L^{(1)}(\theta)$ and $v_L^{(2)}(\theta)$ with θ in Figs. 5 and 6 respectively, whereas the underlying coin operator is \mathcal{X}_θ , $-\pi \leq \theta \leq \pi$.

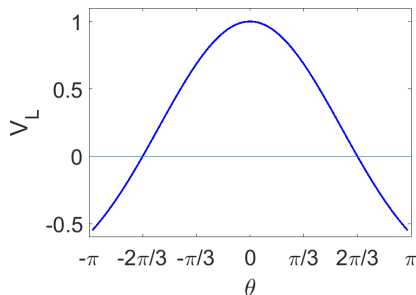


FIG. 5. The velocity $v_L^{(1)}(\theta)$ for the one-parameter family of quantum walks defined by the coin class \mathcal{X}_θ . The velocity of the left traveling probability peak takes the maximal value 1 at $\theta = 0$ and when $|\theta|$ increases it decreases and becomes 0 at $\theta = \pm 2\pi/3$. $v_L^{(1)}(\theta)$ takes a negative value for $|\theta| > 2\pi/3$. The curve for peak velocity is symmetric about the vertical line through $\theta = 0$. For the Grover walk, $v_L^{(1)}(\theta)$ attains the value $-\frac{1}{\sqrt{3}}$, i.e., $v_L^{(1)}(\pi) = v_L^{(1)}(-\pi) = -\frac{1}{\sqrt{3}}$.

In Fig. 7, we plot the probability distributions of the Grover walk for different positions of the walker after three certain time steps.

Figure 8 shows the probability distributions of the walks after time $t = 50$ at different position of the walker with some coins from \mathcal{X}_θ .

From Fig. 5 we see $|v_L^{(1)}(\frac{\pi}{2})| < |v_L^{(1)}(\pi)|$. Accordingly, in Fig. 8, the right and left peaks travel slower than the Grover walk in Fig. 7 through the line, whereas the initial state is $(\frac{1}{\sqrt{2}}, 0, \frac{1}{\sqrt{2}})$ and $t = 50$ for both the cases. Indeed, it is to be noted that, unlike the Grover coin, the coins \mathcal{X}_θ , $\theta = \frac{\pi}{2}, -\frac{\pi}{2}$ are not symmetric, which cause the asymmetric probability distributions with respect to the position $m = 0$.

Now we see in Fig. 9 the probability distribution of the walk with coin from \mathcal{X}_θ with time changes, at a certain position of the walker on the line.

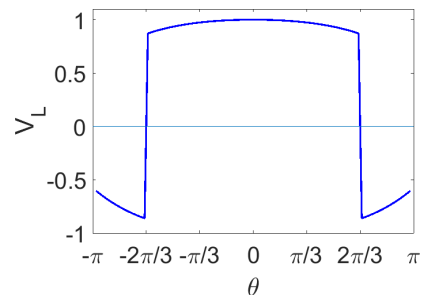


FIG. 6. The velocity $v_L^{(2)}(\theta)$ for the one-parameter family of quantum walks defined by the coin class \mathcal{X}_θ . We see $v_L^{(2)}(\theta)$ attains positive values for $-2\pi/3 < \theta < 2\pi/3$ and take maximum value 1 at $\theta = 0$. For the Grover walk $v_L^{(2)}(\theta) = -\frac{1}{\sqrt{3}}$, $\theta = \pi, -\pi$. Moreover, the peak velocity curve is symmetric about the vertical line through $\theta = 0$. There is a certain jump discontinuity in the peak velocity curve at $\theta = \pm 2\pi/3$. However, the peak velocity $v_L^{(2)}(\theta)$ is not feasible to carry out.

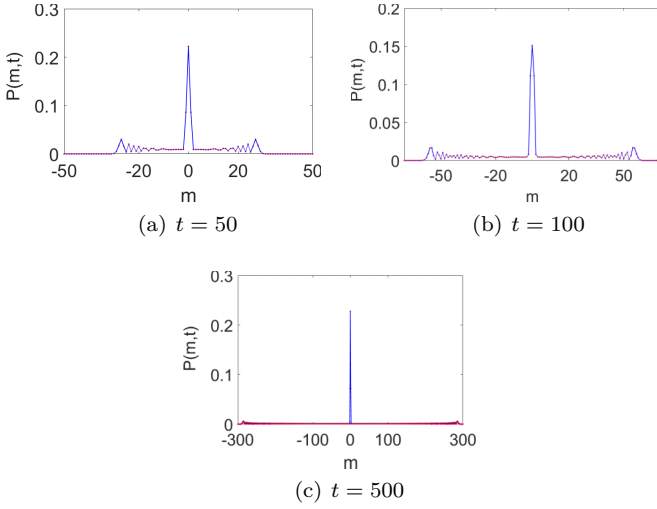


FIG. 7. The probability distribution of the Grover walk after time steps $t = 50$, $t = 100$, and $t = 500$ with initial state $(\frac{1}{\sqrt{2}}, 0, \frac{1}{\sqrt{2}})$. Clearly the probability distribution contains three dominant peaks whose positions are determined by the velocities $v_L^{(1)}(\pi) = -\frac{1}{\sqrt{3}}$, $v_S^{(1)}(\pi) = 0$, $v_R^{(1)}(\pi) = \frac{1}{\sqrt{3}}$. In panel (a), the peak positions correspond to $-27, 0, 27$ and in panel (b), the peak positions appear at $-56, 56, 0$. As time increases we see that the probability values at the peaks diminish gradually. The peak at the origin does not propagate with time, which emphasizes the localization of the Grover walk.

In Fig. 9 we plot the probability of the walker to be at position $m = 0$, over time. Starting from $m = 0$, the quantum walk with coins from \mathcal{X}_θ propagates to other vertices of the line with time. However, the probability to localize (i.e., to remain at $m = 0$) converges to a constant as t increases.

B. With coin operators $C \in \mathcal{Y}_\theta$

Now we consider the walk with coins from \mathcal{Y}_θ , while for $x = (2 \cos \theta - 1)/3$, by Theorem III.5 the eigenvalues of $\tilde{U}_Y(k)$ are $\lambda_j = e^{i\omega_j(k)}$, $j = 1, 2, 3$ where $\omega_1(k) = \pi$, $\omega_2(k) = -\omega_3(k) = \omega(k)$ with $\cos \omega(k) = -\frac{1}{3}(1 - \cos k) - \cos \theta(1 - 2 \cos k)/3$. Here also the eigenvalue $\lambda_1 = -1$ is independent of wave number k and hence the walk shows localization.

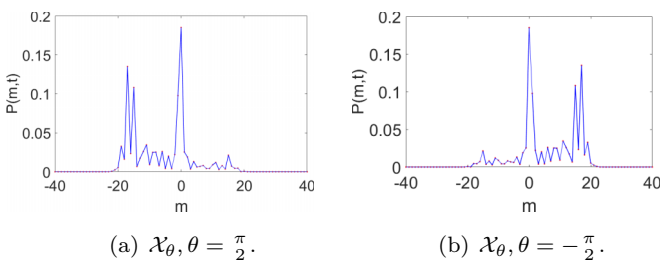


FIG. 8. The probability distribution of the walk using coins from \mathcal{X}_θ for $\theta = \frac{\pi}{2}$ and $\theta = -\frac{\pi}{2}$ after $t = 50$ time steps with the initial state $(\frac{1}{\sqrt{2}}, 0, \frac{1}{\sqrt{2}})$. The peaks on the left and the right side move with velocities $v_{L,R}^{(1)}(\frac{\pi}{2}) = v_{L,R}^{(1)}(-\frac{\pi}{2}) \approx \mp 0.3568$ and appear at positions $T v_{L,R}^{(1)}(\frac{\pi}{2}) = T v_{L,R}^{(1)}(-\frac{\pi}{2}) \approx \mp 17$. Here the probability distribution curves spread much slower in compared with the Grover walk shown in Fig. 7.

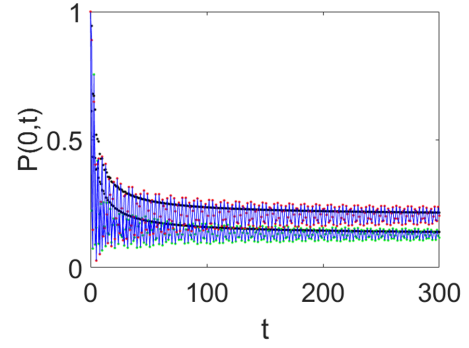


FIG. 9. The probability distribution of the walker with time at the origin $m = 0$, starting with the initial state $(\frac{1}{\sqrt{2}}, 0, \frac{1}{\sqrt{2}})$, while the coins are \mathcal{X}_θ for $\theta = \pi, \frac{\pi}{2}$. The red- and green-colored nodes correspond to $\theta = \pi$ and $\theta = \frac{\pi}{2}$, respectively. Here the black dotted curves passing through the probability distributions are the averaged probabilities of the corresponding walks. It looks apparently that, as time propagates, the averaged probabilities of the walks at $m = 0$ with the Grover coin \mathcal{X}_π and with coin $\mathcal{X}_{\frac{\pi}{2}}$ converge to 0.2 and 0.13.

Similarly as the case \mathcal{X}_θ we determine the peak velocities using the coin operators from \mathcal{Y}_θ . For $\theta = \pi, -\pi$, \mathcal{Y}_θ becomes $-I_3$, so that $\omega_2(k), \omega_3(k) = \pm k$ and $v_R = 1, v_L = -1$. Similarly, if $\theta = \frac{\pi}{3}$ or $\theta = -\frac{\pi}{3}$ we get permutation matrices $P_{(132)} \in \mathcal{Y}_\theta$ or $-P_{(123)} \in \mathcal{Y}_\theta$, respectively. For both the cases peak velocities are zero. If $\theta = 0$ the coin operator is the negative times Grover matrix, whose right and left peak velocities are $-\frac{1}{\sqrt{3}}$ and $\frac{1}{\sqrt{3}}$, respectively.

Now We get that $\frac{d^2 \omega_2(k)}{dk^2}$ vanishes for

$$k_0^1 = \pi - \arccos \left(\frac{5 \cos \theta - 7 + 3\sqrt{\cos^2 \theta - 6 \cos \theta + 5}}{2(2 \cos \theta - 1)} \right)$$

and

$$k_0^2 = \pi - \arccos \left(\frac{5 \cos \theta - 7 - 3\sqrt{\cos^2 \theta - 6 \cos \theta + 5}}{2(2 \cos \theta - 1)} \right),$$

for $(2 \cos \theta - 1) \neq 0, -3, 1$, i.e., $\theta \neq \frac{\pi}{3}, -\frac{\pi}{3}, \pi, -\pi, 0$.

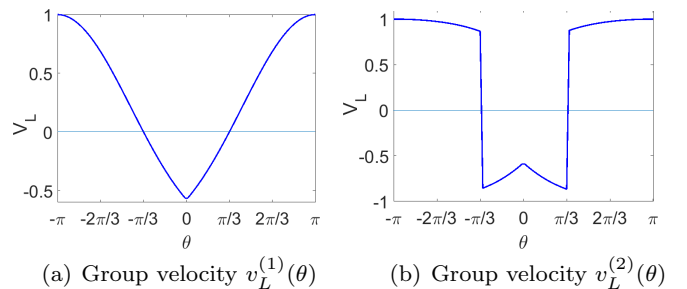


FIG. 10. $v_L^{(1)}(\theta)$ and $v_L^{(2)}(\theta)$ for the one-parameter family of quantum walks defined by the coin class \mathcal{Y}_θ . At $\theta = 0$ $v_L^{(1)}(0)$ attains the value $-\frac{1}{\sqrt{3}}$. $v_L^{(1)}(\theta)$ takes the maximal value 1 at $\theta = -\pi, \pi$ and is negative for $|\theta| < 2\pi/3$. In panel (a), the velocity increases as $|\theta|$ increases and becomes 0 at $\theta = \pm\pi/3$. Whereas in panel (b), the velocity decreases as $|\theta|$ increases and there is a discontinuity of the left peak velocity curve at $\theta = \pm\pi/3$, in contrast with panel (a).

Then the group velocities

$$\frac{d\omega_2(k)}{dk} = -\frac{d\omega_3(k)}{dk} = \frac{\frac{1}{3} \sin k(1 - 2 \cos \theta)}{\sqrt{1 - \left[\frac{1}{3}(1 - \cos k) + \frac{1}{3} \cos \theta(1 + 2 \cos k)\right]^2}}$$

at the stationary points k_1^0 and k_2^0 are as follows:

$$v_L^{(1)}(\theta) = \left. \frac{d\omega_2(k)}{dk} \right|_{k=k_1^0} = \begin{cases} -\frac{1}{3} \sqrt{\frac{9\sqrt{\cos^2 \theta - 6 \cos \theta + 5} + (15 \cos \theta - 21)}{\cos^2 \theta - 6 \cos \theta + 5 + (\cos \theta - 3)}} & \text{if } -\frac{\pi}{3} < \theta < \frac{\pi}{3} \\ \frac{1}{3} \sqrt{\frac{9\sqrt{\cos^2 \theta - 6 \cos \theta + 5} + (15 \cos \theta - 21)}{\cos^2 \theta - 6 \cos \theta + 5 + (\cos \theta - 3)}} & \text{if } -\pi < \theta < -\frac{\pi}{3}, \frac{\pi}{3} < \theta < \pi, \end{cases}$$

$$v_R^{(1)}(\theta) = -v_L^{(1)}(\theta),$$

$$v_L^{(2)}(\theta) = \left. \frac{d\omega_2(k)}{dk} \right|_{k=k_2^0} = \begin{cases} -\frac{1}{3} \sqrt{\frac{9\sqrt{\cos^2 \theta - 6 \cos \theta + 5} - (15 \cos \theta - 21)}{\cos^2 \theta - 6 \cos \theta + 5 - (\cos \theta - 3)}} & \text{if } -\frac{\pi}{3} < \theta < \frac{\pi}{3} \\ \frac{1}{3} \sqrt{\frac{9\sqrt{\cos^2 \theta - 6 \cos \theta + 5} - (15 \cos \theta - 21)}{\cos^2 \theta - 6 \cos \theta + 5 - (\cos \theta - 3)}} & \text{if } -\pi < \theta < -\frac{\pi}{3}, \frac{\pi}{3} < \theta < \pi, \end{cases}$$

$$v_R^{(2)}(\theta) = -v_L^{(2)}(\theta),$$

whenever $(2 \cos \theta - 1) \neq 0, -3, 1$.

We show the changes in the functional values of $v_L^{(1)}(\theta)$ and $v_L^{(2)}(\theta)$ with θ in Fig. 10.

Next, Fig. 11 shows the probability distributions of the walk with negative times the Grover coin, i.e., $\theta = 0$, at different position of the walker after three certain time steps.

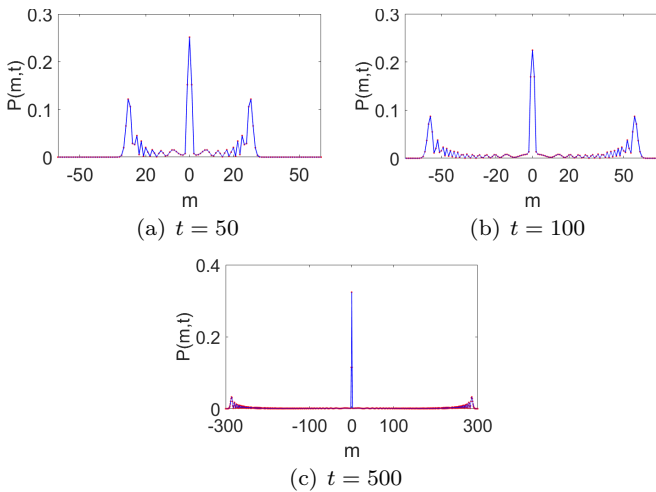


FIG. 11. The probability distribution corresponding to negative of the Grover coin after time steps $t = 50, 100, 500$ with initial state $(\frac{1}{\sqrt{3}}, \frac{1}{\sqrt{3}}, \frac{1}{\sqrt{3}})$. Clearly the probability distribution contains three dominant peaks whose positions are determined by the velocities $v_L^{(1)}(0) = \frac{1}{\sqrt{3}}, v_S^{(1)}(0) = 0, v_R^{(1)}(0) = -\frac{1}{\sqrt{3}}$. In panel (a), the peak positions correspond to $-28, 0, 28$ and in panel (b), the peak positions appear at $-56, 0, 56$. In contrast with panels (a) and (b) for the probability distribution in panel (c) corresponds to a large time step $t = 500$, the left and right peaks take small probability values. In all the figures the central peak at the origin does not propagate with time, which emphasizes the localization of the walk with negative Grover coin.

Figure 12 shows the probability distributions of the walks after time $t = 50$ at different position of the walker with some coins from \mathcal{Y}_θ .

From Fig. 10 we see $|v_L^{(1)}(\frac{\pi}{6})| < |v_L^{(1)}(0)|$. Hence in Fig. 12 the right and left peaks travel slower than the walk in Fig. 11 through the line, whereas the initial state is $(\frac{1}{\sqrt{3}}, \frac{1}{\sqrt{3}}, \frac{1}{\sqrt{3}})$ and $t = 50$ for both the cases. In contrast with the walk with negative Grover coin, the walks with coins $\mathcal{Y}_\theta, \theta = \frac{\pi}{6}, -\frac{\pi}{6}$ have asymmetric probability distributions with respect to the position $m = 0$.

V. CONCLUSION

We have proved two limit theorems for three-state quantum walks on one-dimensional lattices when the coin operators are considered as generalized Grover operators which are recently introduced in the literature by characterizing orthogonal matrices of dimension 3×3 that can be written as a linear sum of permutation matrices. Furthermore, we have analyzed the localization properties of the walks by using the obtained

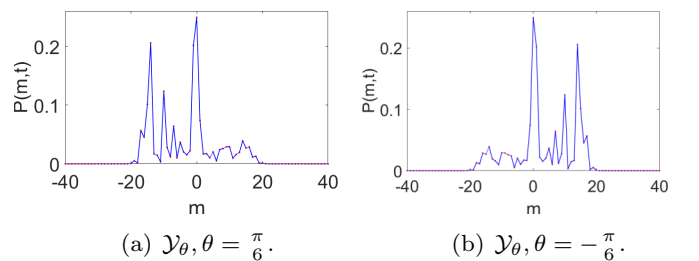


FIG. 12. The probability distribution of the walk using coins from \mathcal{Y}_θ for $\theta = \frac{\pi}{6}$ and $\theta = -\frac{\pi}{6}$ after $t = 50$ time steps with the initial state $(\frac{1}{\sqrt{3}}, \frac{1}{\sqrt{3}}, \frac{1}{\sqrt{3}})$. The peaks on the left and the right side move with velocities $v_{L,R}^{(1)}(\frac{\pi}{6}) = v_{L,R}^{(1)}(-\frac{\pi}{6})$ and appear at positions $T v_{L,R}^{(1)}(\frac{\pi}{6}) = T v_{L,R}^{(1)}(-\frac{\pi}{6}) \approx \mp 14$. Clearly, the probability distribution curves spread much slower in compared with the walk shown in Fig. 11.

formula of probability measure of finding the walker at any position with a given generic initial state. Indeed, we have shown that the walks show localization phenomena generically, and we also have classified the initial states for which the walks do not show localization phenomena when the initial position is assumed to be the origin. In support of these results we have analyzed peak velocities associated with the limiting distributions of the walks. All our analytical results have been thoroughly corroborated with numerical examples.

Our results can be used to determine how fast the quantum walks described here converge to their time-averaged limiting distribution. As mentioned earlier, this phenomena, known as mixing, has been crucial in analyzing the running times of several quantum algorithms. In fact, it has been demonstrated that discrete-time quantum walks on a one-dimensional lattice with a Hadamard coin mixes quadratically faster than its classical counterpart. It would be interesting to investigate whether this speedup is retained for quantum walks with the

parametrized coins introduced here. Other topologies, such as higher dimensional lattices, can also be explored in this regard. Another future plan of our research includes developing quantum circuit models for the proposed quantum walks.

ACKNOWLEDGMENTS

A.M. thanks the Council for Scientific and Industrial Research (CSIR), India for financial support in the form of a junior-senior research fellowship. R.S.S. acknowledges support through Prime Minister Research Fellowship (PMRF), Government of India. S.C. acknowledges IIT Kharagpur for providing the necessary support for his visit to IIT Kharagpur. S.C. acknowledges funding from Science and Engineering Research Board, Department of Science and Technology (SERB-DST), Government of India under Grant No. SRG/2022/000354. S.C. also acknowledges funding from IIT Hyderabad under the Faculty Seed Grant.

APPENDIX A: DERIVATION RELATED TO LIMIT THEOREMS

Below we derive a compact expression for the quantum state $|\psi(m, t)\rangle$, the probability amplitude vector as defined in Eq. (2) when the coin operator $C \in \mathcal{X}$. A similar expression can be obtained for coins in \mathcal{Y} .

$$\begin{aligned} & \sum_{j=2}^3 \frac{1}{2\pi} \int_{-\pi}^{\pi} e^{i[-km+w_j(k)t]} \langle v_j(k) | \Psi(k, 0) | v_j(k) \rangle dk \\ &= \frac{1}{2\pi} \int_{-\pi}^{\pi} \frac{1}{\|f_2(\omega(k))\|^2} \left(\left[\frac{y + (1-x-y)e^{i\omega(k)}}{(1-x-y) + ye^{i[\omega(k)-k]}} , 1, \frac{1-x-y + ye^{i\omega(k)}}{y + (1-x-y)e^{i[\omega(k)+k]}} \right]^T \right. \\ & \quad \times \left. \left[\alpha \frac{y + (1-x-y)e^{-i\omega(k)}}{(1-x-y) + ye^{-i[\omega(k)-k]}} + \beta + \gamma \frac{1-x-y + ye^{-i\omega(k)}}{y + (1-x-y)e^{-i[\omega(k)+k]}} \right] e^{i[\omega(k)t-km]} \right) dk \\ &+ \frac{1}{2\pi} \int_{-\pi}^{\pi} \frac{1}{\|f_3(-\omega(k))\|^2} \left(\left[\frac{y + (1-x-y)e^{-i\omega(k)}}{(1-x-y) + ye^{-i[\omega(k)+k]}} , 1, \frac{1-x-y + ye^{-i\omega(k)}}{y + (1-x-y)e^{-i[\omega(k)-k]}} \right]^T \right. \\ & \quad \times \left. \left[\alpha \frac{y + (1-x-y)e^{i\omega(k)}}{(1-x-y) + ye^{i[\omega(k)+k]}} + \beta + \gamma \frac{1-x-y + ye^{i\omega(k)}}{y + (1-x-y)e^{i[\omega(k)-k]}} \right] e^{i[-\omega(k)t-km]} \right) dk \\ &= [a_{11}\alpha + a_{12}\beta + a_{13}\gamma, a_{21}\alpha + a_{22}\beta + a_{23}\gamma, a_{31}\alpha + a_{32}\beta + a_{33}\gamma]^T. \end{aligned}$$

Then comparing both sides for the coefficients of α, β, γ we get $a_{ij}, i, j \in \{1, 2, 3\}$. Here we derive a_{11} and the other a_{ij} can be obtained similarly.

By Theorem III.1 $\|f_2(\omega(k))\|^2 = \|f_3(-\omega(k))\|^2$ and hence

$$a_{11} = \frac{1}{2\pi} \int_{-\pi}^{\pi} \frac{1}{\|f_2(\omega(k))\|^2} \left(\left| \frac{y + (1-x-y)e^{i\omega(k)}}{(1-x-y) + ye^{i[\omega(k)-k]}} \right|^2 e^{i[\omega(k)t-km]} + \left| \frac{y + (1-x-y)e^{-i\omega(k)}}{(1-x-y) + ye^{-i[\omega(k)+k]}} \right|^2 e^{i[-\omega(k)t+km]} \right) dk.$$

Simplifying the above expression it becomes

$$a_{11} = \frac{1}{2\pi} \int_{-\pi}^{\pi} e^{-ikm} \left(\frac{1+x-2x \cos \omega(k)}{1+x-2x \cos [\omega(k)-k]} e^{i\omega(k)t} + \frac{1+x-2x \cos \omega(k)}{1+x-2x \cos [\omega(k)+k]} e^{-i\omega(k)t} \right) dk.$$

Clearly the above expression simplifies a_{11} to the form $\frac{1}{2\pi} \int_{-\pi}^{\pi} G(\omega(k), k) \cos(\omega(k)t) \cos(km) dk$, where $G(\omega(k), k)$ is a quotient function which is a continuous functions of k . Hence for all coins in \mathcal{X} which are not permutation matrices i.e., $x \neq 0, 1$, we get $G(\omega(k), k)$ is Riemann integrable as well as Lebesgue integrable.

Thus using the Riemann-Lebesgue Lemma we say $a_{11} \approx 0$ as $t \rightarrow \infty$. Similarly it can be done for other $a_{ij}, i, j \in \{1, 2, 3\}$.

APPENDIX B: DERIVATION RELATED TO LOCALIZATION CONDITION USING THE DEFINITION GIVEN IN Ref. [46]

Recall that the localization condition for a DTQW as proposed in Ref. [46] is $\sum_{m \in \mathbb{Z}} \lim_{t \rightarrow \infty} P(m, t)$ to be positive.

Then, for coins in \mathcal{X} , the parameter ν as mentioned in Theorem III.3, is such that $-5 + 2\sqrt{6} \leq \nu < 1$ for $x \neq 0, 1$, so that $1 - \nu^2 \neq 0$. Suppose $x \neq 0, 1$ and $T_1 = \alpha(1 - x - y) + \beta(1 + x) + \gamma y$, $T_2 = \alpha y - \beta x$, $T_3 = -\beta x + \gamma(1 - x - y)$. Then considering the approximation of $\lim_{t \rightarrow \infty} P(m, t)$ in Theorem III.3, taking sum over all the positions on the line, we obtain

$$\begin{aligned} \sum_{m \in \mathbb{Z}} \lim_{t \rightarrow \infty} P(m, t) &= \frac{1}{3(1-x)(x+3)} \left[2 \left\{ (|A|^2 + |B|^2) \sum_{m \in \mathbb{Z}} \nu^{2|m|} + 2\text{Re}(A\bar{B}) \sum_{m \in \mathbb{Z}} \nu^{|m|+|m+1|} \right\} \right. \\ &\quad + \left\{ (|T_1|^2 + |T_2|^2 + |T_3|^2) \sum_{m \in \mathbb{Z}} \nu^{2|m|} + 2(\text{Re}(T_1\bar{T}_2) + \text{Re}(T_1\bar{T}_3)) \sum_{m \in \mathbb{Z}} \nu^{|m|+|m+1|} \right\} \\ &\quad \left. + \left\{ 2\text{Re}(T_2\bar{T}_3) \sum_{m \in \mathbb{Z}} \nu^{|-m+1|+|m+1|} \right\} \right] \\ &= \frac{1}{3(1-x)(x+3)} \left[\left\{ [2(|A|^2 + |B|^2) + (|T_1|^2 + |T_2|^2 + |T_3|^2)] \sum_{m \in \mathbb{Z}} \nu^{2|m|} \right\} \right. \\ &\quad + \left\{ 2[\text{Re}(A\bar{B}) + \text{Re}(T_1\bar{T}_2) + \text{Re}(T_1\bar{T}_3)] \sum_{m \in \mathbb{Z}} \nu^{|m|+|m+1|} \right\} + \left\{ 2\text{Re}(T_2\bar{T}_3) \sum_{m \in \mathbb{Z}} \nu^{|-m+1|+|m+1|} \right\} \right] \\ &= \frac{1}{3(1-x)(x+3)} \left[\frac{1+\nu^2}{1-\nu^2} \{ 2|A|^2 + 2|B|^2 + |T_1|^2 + |T_2|^2 + |T_3|^2 \} \right. \\ &\quad + 2\nu^{-1} [\text{Re}(A\bar{B}) + \text{Re}(T_1\bar{T}_2) + \text{Re}(T_1\bar{T}_3)] + 2\text{Re}(T_2\bar{T}_3) \left. \right] - 2\nu^{-1} [\text{Re}(A\bar{B}) + \text{Re}(T_1\bar{T}_2) + \text{Re}(T_1\bar{T}_3)] \\ &\quad - 2(1-\nu^2)\text{Re}(T_2\bar{T}_3) \left. \right] \\ &= \frac{1}{3(1-x)(x+3)} \left[\frac{1+\nu^2}{1-\nu^2} (2|A|^2 + 2|B|^2 + |T_1|^2 + |T_2|^2 + |T_3|^2) + \frac{4\nu}{1-\nu^2} [\text{Re}(A\bar{B}) + \text{Re}(T_1\bar{T}_2) + \text{Re}(T_1\bar{T}_3)] \right. \\ &\quad \left. + 2\nu^2 \frac{3-\nu^2}{1-\nu^2} \text{Re}(T_2\bar{T}_3) \right]. \end{aligned}$$

Furthermore, for coins in \mathcal{Y} , in order to derive a criterion for localization and to analyze the dependency of it on the initial state, we obtain from Theorem III.6 for $x \neq 0, -1$,

$$\begin{aligned} \sum_{m \in \mathbb{Z}} \lim_{t \rightarrow \infty} P(m, t) &= \frac{1}{3(1+x)(3-x)} \left[\frac{1+\mu^2}{1-\mu^2} (2|D|^2 + 2|E|^2 + |S_1|^2 + |S_2|^2 + |S_3|^2) \right. \\ &\quad \left. + \frac{4\mu}{1-\mu^2} [\text{Re}(D\bar{E}) + \text{Re}(S_1\bar{S}_2) + \text{Re}(S_1\bar{S}_3)] + 2\mu^2 \frac{3-\mu^2}{1-\mu^2} \text{Re}(S_2\bar{S}_3) \right]. \end{aligned}$$

where $S_1 = \alpha(1 + x + y) + \beta(1 - x) - \gamma y$, $S_2 = -\alpha y + \beta x$, $S_3 = \beta x + \gamma(1 + x + y)$, and $-5 + 2\sqrt{6} \leq \mu < 1$, $\mu^2 < 1$.

-
- [1] D. Aharonov, A. Ambainis, J. Kempe, and U. Vazirani, Quantum walks on graphs, in *Proceedings of the Thirty-Third Annual ACM Symposium on Theory of Computing* (Association for Computing Machinery, New York, NY, 2001), pp. 50–59.
- [2] A. M. Childs, Universal Computation by Quantum Walk, *Phys. Rev. Lett.* **102**, 180501 (2009).
- [3] N. B. Lovett, S. Cooper, M. Everitt, M. Trevers, and V. Kendon, Universal quantum computation using the discrete-time quantum walk, *Phys. Rev. A* **81**, 042330 (2010).
- [4] A. M. Childs, R. Cleve, E. Deotto, E. Farhi, S. Gutmann, and D. A. Spielman, Exponential algorithmic speedup by a quantum walk, in *Proceedings of the Thirty-Fifth Annual ACM Symposium on Theory of Computing* (Association for Computing Machinery, New York, NY, 2003), pp. 59–68.
- [5] A. Ambainis, Quantum walk algorithm for element distinctness, *SIAM J. Comput.* **37**, 210 (2007).
- [6] F. Magniez, A. Nayak, J. Roland, and M. Santha, Search via quantum walk, *SIAM J. Comput.* **40**, 142 (2011).
- [7] S. Apers, S. Chakraborty, L. Novo, and J. Roland, Quadratic speedup for spatial search by continuous-time quantum walk, [arXiv:2112.12746](https://arxiv.org/abs/2112.12746).
- [8] M. Mohseni, P. Rebentrost, S. Lloyd, and A. Aspuru-Guzik,

- Environment-assisted quantum walks in photosynthetic energy transfer, *J. Chem. Phys.* **129**, 174106 (2008).
- [9] P. Reberstrost, M. Mohseni, I. Kassal, S. Lloyd, and A. Aspuru-Guzik, Environment-assisted quantum transport, *New J. Phys.* **11**, 033003 (2009).
- [10] A. W. Chin, A. Datta, F. Caruso, S. F. Huelga, and M. B. Plenio, Noise-assisted energy transfer in quantum networks and light-harvesting complexes, *New J. Phys.* **12**, 065002 (2010).
- [11] D. A. Meyer, From quantum cellular automata to quantum lattice gases, *J. Stat. Phys.* **85**, 551 (1996).
- [12] E. Farhi and S. Gutmann, Quantum computation and decision trees, *Phys. Rev. A* **58**, 915 (1998).
- [13] S. E. Venegas-Andraca, Quantum walks: A comprehensive review, *Quantum Inf. Process.* **11**, 1015 (2012).
- [14] S. Chakraborty, L. Novo, and J. Roland, Finding a marked node on any graph via continuous-time quantum walks, *Phys. Rev. A* **102**, 022227 (2020).
- [15] Y. Atia and S. Chakraborty, Improved upper bounds for the hitting times of quantum walks, *Phys. Rev. A* **104**, 032215 (2021).
- [16] D. Aharonov, W. Van Dam, J. Kempe, Z. Landau, S. Lloyd, and O. Regev, Adiabatic quantum computation is equivalent to standard quantum computation, *SIAM Rev.* **50**, 755 (2008).
- [17] L. Caha, Z. Landau, and D. Nagaj, Clocks in Feynman's computer and Kitaev's local Hamiltonian: Bias, gaps, idling, and pulse tuning, *Phys. Rev. A* **97**, 062306 (2018).
- [18] P. C. Richter, Quantum speedup of classical mixing processes, *Phys. Rev. A* **76**, 042306 (2007).
- [19] S. Chakraborty, K. Luh, and J. Roland, How Fast Do Quantum Walks Mix?, *Phys. Rev. Lett.* **124**, 050501 (2020).
- [20] S. Chakraborty, K. Luh, and J. Roland, Analog quantum algorithms for the mixing of Markov chains, *Phys. Rev. A* **102**, 022423 (2020).
- [21] N. Inui, Y. Konishi, and N. Konno, Localization of two-dimensional quantum walks, *Phys. Rev. A* **69**, 052323 (2004).
- [22] N. Inui and N. Konno, Localization of multi-state quantum walk in one dimension, *Phys. A (Amsterdam, Neth.)* **353**, 133 (2005).
- [23] N. Inui, N. Konno, and E. Segawa, One-dimensional three-state quantum walk, *Phys. Rev. E* **72**, 056112 (2005).
- [24] E. Segawa, Localization of quantum walks induced by recurrence properties of random walks, *J. Comp. Theor. Nanosci.* **10**, 1583 (2013).
- [25] B. Kollár, T. Kiss, and I. Jex, Strongly trapped two-dimensional quantum walks, *Phys. Rev. A* **91**, 022308 (2015).
- [26] T. Tate, Eigenvalues, absolute continuity and localizations for periodic unitary transition operators, *Infin. Dimens. Anal. Quantum Probab. Relat. Top.* **22**, 1950011 (2019).
- [27] N. Konno, Localization of an inhomogeneous discrete-time quantum walk on the line, *Quantum Inf. Process.* **9**, 405 (2010).
- [28] R. S. Sarkar, A. Mandal, and B. Adhikari, Periodicity of lively quantum walks on cycles with generalized Grover coin, *Lin. Alg. Appl.* **604**, 399 (2020).
- [29] B. Kollár, M. Štefaňák, T. Kiss, and I. Jex, Recurrences in three-state quantum walks on a plane, *Phys. Rev. A* **82**, 012303 (2010).
- [30] B. Kollár, A. Gilyén, I. Tkáčová, T. Kiss, I. Jex, and M. Štefaňák, Complete classification of trapping coins for quantum walks on the two-dimensional square lattice, *Phys. Rev. A* **102**, 012207 (2020).
- [31] M. Štefaňák, I. Bezděková, and I. Jex, Continuous deformations of the Grover walk preserving localization, *Eur. Phys. J. D* **66**, 142 (2012).
- [32] A. Mandal and B. Adhikari, A characterization of orthogonal permutative matrices of order 4, *Lin. Alg. Appl.* **654**, 102 (2022).
- [33] K. Watabe, N. Kobayashi, M. Katori, and N. Konno, Limit distributions of two-dimensional quantum walks, *Phys. Rev. A* **77**, 062331 (2008).
- [34] A. Mandal, R. S. Sarkar, and B. Adhikari, Localization of two-dimensional quantum walks defined by generalized grover coins, [arXiv:2103.00515](https://arxiv.org/abs/2103.00515).
- [35] C. Di Franco, M. Mc Gettrick, T. Machida, and T. Busch, Alternate two-dimensional quantum walk with a single-qubit coin, *Phys. Rev. A* **84**, 042337 (2011).
- [36] Y. Ide, N. Konno, T. Machida, and E. Segawa, Return probability of one-dimensional discrete-time quantum walks with final-time dependence, *Quantum Inf. Comput.* **11**, 761 (2011).
- [37] M. Štefaňák, I. Bezděková, and I. Jex, Limit distributions of three-state quantum walks: The role of coin eigenstates, *Phys. Rev. A* **90**, 012342 (2014).
- [38] T. Chen and X. Zhang, The defect-induced localization in many positions of the quantum random walk, *Sci. Rep.* **6**, 25767 (2016).
- [39] M. Bataille, Quantum circuits of CNOT gates: Optimization and entanglement, *Quantum Inf. Process.* **21**, 269 (2022).
- [40] P. L. Knight, E. Roldán, and J. E. Sipe, Quantum walk on the line as an interference phenomenon, *Phys. Rev. A* **68**, 020301(R) (2003).
- [41] A. Kempf and R. Portugal, Group velocity of discrete-time quantum walks, *Phys. Rev. A* **79**, 052317 (2009).
- [42] A. C. Orthey Jr and E. P. M. Amorim, Connecting velocity and entanglement in quantum walks, *Phys. Rev. A* **99**, 032320 (2019).
- [43] M. Štefaňák, T. Kiss, and I. Jex, Recurrence properties of unbiased coined quantum walks on infinite d -dimensional lattices, *Phys. Rev. A* **78**, 032306 (2008).
- [44] C. K. Ko, E. Segawa, and H. J. Yoo, One-dimensional three-state quantum walks: Weak limits and localization, *Infin. Dimens. Anal. Quantum Probab. Relat. Top.* **19**, 1650025 (2016).
- [45] M. Štefaňák, I. Jex, and T. Kiss, Recurrence and Pólya Number of Quantum Walks, *Phys. Rev. Lett.* **100**, 020501 (2008).
- [46] T. Machida, Limit theorems of a 3-state quantum walk and its application for discrete uniform measures, [arXiv:1404.1522](https://arxiv.org/abs/1404.1522).
- [47] E. Segawa and A. Suzuki, Generator of an abstract quantum walk, *Quantum Stud.: Math. Found.* **3**, 11 (2016).
- [48] A. Klappenecker and M. Roetteler, Quantum software reusability, *Int. J. Found. Comput. Sci.* **14**, 777 (2003).
- [49] T. Machida and C. M. Chandrashekar, Localization and limit laws of a three-state alternate quantum walk on a two-dimensional lattice, *Phys. Rev. A* **92**, 062307 (2015).
- [50] E. M. Stein and R. Shakarchi, *Fourier Analysis: An Introduction* (Princeton University Press, 2011), Vol. 1.
- [51] R. Wong, *Asymptotic Approximations of Integrals* (SIAM, Philadelphia, 2001).